STUK

March 1999

The influence of modified water chemistries on metal oxide films, activity build-up and stress corrosion cracking of structural materials in nuclear power plants

K. Mäkelä, T. Laitinen, M. Bojinov
VTT Manufacturing Technology

In STUK this study was supervised by **Seija Suksi**

STUK • SÄTEILYTURVAKESKUS • STRÅLSÄKERHETSCENTRALEN
RADIATION AND NUCLEAR SAFETY AUTHORITY

The conclusions presented in the STUK report series are those of the authors
and do not necessarily represent the official position of STUK.

ABSTRACT

The primary coolant oxidises the surfaces of construction materials in nuclear power plants. The properties of the oxide films influence significantly the extent of incorporation of activated corrosion products into the primary circuit surfaces, which may cause additional occupational doses for the maintenance personnel. The physical and chemical properties of the oxide films play also an important role in different forms of corrosion observed in power plants.

This report gives a short overview of the factors influencing activity build-up and corrosion phenomena in nuclear power plants. Furthermore, the most recent modifications in the water chemistry to decrease these risks are discussed. A special focus is put on zinc water chemistry, and a preliminary discussion on the mechanism via which zinc influences activity build-up is presented. Even though the exact mechanisms by which zinc acts are not yet known, it is assumed that Zn may block the diffusion paths within the oxide film. This reduces ion transport through the oxide films leading to a reduced rate of oxide growth. Simultaneously the number of available adsorption sites for ^{60}Co is also reduced.

The current models for stress corrosion cracking assume that the anodic and the respective cathodic reactions contributing to crack growth occur partly on or in the oxide films. The rates of these reactions may control the crack propagation rate and therefore, the properties of the oxide films play a crucial role in determining the susceptibility of the material to stress corrosion cracking.

Finally, attention is paid also on the novel techniques which can be used to mitigate the susceptibility of construction materials to stress corrosion cracking.

TIIVISTELMÄ

Ydinvoimalaitosten primääripiirin rakennemateriaalien pinnat hapettuvat jäähdytysveden vaikutuksesta. Syntyvien oksidifilmien ominaisuudet vaikuttavat merkittävästi radioaktiivisten osaslajien kerääntymiseen primääripiirin pinnoille, mikä taas vaikuttaa henkilökunnan saamiin säteilyannoksiin huoltoseisokkien aikana. Oksidifilmien fysikaalisilla ja kemiallisilla ominaisuuksilla on myös suuri vaikutus eri korroosioilmiöihin ydinvoimalaitoksissa.

Tässä kirjallisuustyössä on esitetty lyhyt yhteenveto tekijöistä, jotka vaikuttavat aktiivisuuden kerääntymiseen ja tiettyihin korroosioilmiöihin ydinvoimaloissa. Lisäksi työssä käsitellään uusimpia tapoja modifioida voimaloiden vesikemiaa tarkoituksena pienentää edellä mainittujen ilmiöiden riskiä. Sinkkivesikemiaa on painotettu erityisesti. Vaikka sinkin tarkka vaikutusmekanismi aktiivisuuden kerääntymisen pienentämisessä on tuntematon, sinkin voidaan olettaa tukkivan diffuusioreittejä oksidifilmissä. Tämä hidastaa ionien kuljetusta filmissä ja johtaa hitaampaan filmin kasvuun. Samalla myös saatavilla olevien ^{60}Co:n adsorptiopaikkojen määrä pienenee.

Nykyisissä jännityskorroosiomalleissa oletetaan, että särönkasvuun vaikuttavat anodiset ja vastaavat katodiset reaktiot tapahtuvat osittain oksidifilmeissä tai niiden pinnoilla. Näiden reaktioiden nopeudet voivat kontrolloida särönkasvunopeutta, joten oksidifilmien ominaisuuksilla voi olla ratkaiseva merkitys materiaalien jännityskorroosiokestävyyden kannalta. Tässä työssä käsitellään uusimpia tekniikoita, joiden avulla materiaalien jännityskorroosiokestävyyttä voidaan parantaa muuttamalla metallien pinnoille muodostuvien oksidifilmien sähköisiä ominaisuuksia.

CONTENTS

ACKNOWLEDGEMENTS

1 INTRODUCTION

The interaction between the construction materials and the aqueous coolant leads to the oxidation of the primary circuit piping surfaces in nuclear power plants. As a result of the susceptibility of materials to oxidise, different forms of corrosion mechanisms may pose serious hazards to the operation of the plant. Oxide films formed on material surfaces play an important role in uniform corrosion attack, as well as on localised corrosion or stress corrosion cracking. In addition, the properties of oxide films influence the extent of incorporation of active species into the primary circuit materials, which may result in increased occupational doses of radiation for the personnel of the plant.

The main objective of radiation field control in a nuclear power plant is to maintain personnel radiation exposures as low as reasonable achievable (ALARA). The first attempts to achieve exposure savings were mainly obtained by minimising the time spent by workers in radiation fields during maintenance, inspections and refuelling. Another approach is to develop and modify the water chemistry of the plant and thus achieve conditions, under which risks for activity build-up and simultaneously for detrimental corrosion phenomena are minimised. The report by International Atomic Energy Agency (IAEA) co-ordinated research program entitled "Investigation on Water Chemistry Control and Coolant Interaction with Fuel and Primary Circuit Materials in Water Cooled Power Reactors (WACOLIN)" summaries the present philosophy on good coolant chemistry

as follows: "Good reactor coolant chemistry, corrosion control and minimum of activity build-up are indispensable for the optimum performance of nuclear power plants. Without these the system integrity may be jeopardised and the activity transport may create various problems."[1]

In order to maintain good coolant chemistry, extensive water chemistry guidelines have been developed for the pressurised and boiling water reactors (PWR and BWR). Properly controlled water chemistry during steady state operation and shutdowns has led to low corrosion rates of construction materials. Nevertheless, some plant data have shown that despite of following the strict water chemistry guidelines, certain undesirable phenomena, such as increased activity build-up on the primary loop piping surfaces and stress corrosion cracking of in-core components, can still occur. Although further developments in water chemistry in NPPs, e.g. zinc water chemistry, have recently been introduced, it is evident that a proper understanding of the interaction of the coolant and the oxide films on material surfaces in NPPs is not yet available.

The aim of this report is to give a short overview of the factors influencing activity build-up and corrosion phenomena in nuclear power plants. Moreover, the most recent modifications of water chemistries to decrease these risks are discussed. A special focus is on zinc water chemistry, and a preliminary discussion on the mechanism via which zinc influences activity build-up is also reviewed.

2 WATER CHEMISTRIES IN LIGHT WATER REACTORS

Thermal reactors are most commonly used in nuclear power plants. They are categorised according to the coolant, which is used to cool down the reactor itself and also according to the medium which slows down the neutrons formed during the fission reaction. The most common thermal reactor types are the light water reactors which can be either boiling or pressurised water reactors. There are some fundamental differences in the water chemistries of these two types of reactors and therefore a short introduction is given in following chapters.

2.1 Boiling water reactors (BWR)

Steam/water cycle is essentially a closed loop in boiling water reactors (BWR). The water is heated in the reactor core, where a fraction of it is converted into steam. In the upper part of the reactor core steam passes through the steam drier and is transported in main steam line to high and low pressure turbines. Steam starts to condense already in the turbines but condensation mainly occurs in the condensers. After the condensers the water is cleaned by demineralisers and is fed back to the re-circulation loop. To minimise the corrosion product deposition on the fuel cladding surfaces, impurity concentrations in the water circulating in BWRs is kept as low as possible. Therefore, the water conductivity is typically below 0.13 μScm^{-1} during steady-state operation.

Despite of the strict water chemistry guidelines, sensitised microstructure of the primary circuit stainless steels, coupled with residual stresses produces susceptibility to stress corrosion cracking (SCC) in the presence of oxidising species in the coolant.[2] The sensitised microstructures and stresses can not be eliminated in existing plants and therefore, the obvious remedy to prevent intergranular stress corrosion cracking (IGSCC) is to optimise the operational environment further. Laboratory tests and actual power plant measurements indicate that to prevent crack formation and propagation in the BWR stainless steel parts, the corrosion potential (ECP) of primary loop components has to be kept more nega-

tive than -0.230 V_{SHE} in high purity water (conductivity less than 0.3 μScm^{-1}). Despite the rather high volatility of dissolved oxygen and hydrogen peroxide, their contents under normal water chemistry (NWC) conditions in BWR coolant are still about 100–300 ppb (μgkg^{-1}). These oxidising species can shift the corrosion potential of stainless steel parts up to a value of $+0.150$ V_{SHE}, thus supporting stress corrosion cracking. On the other hand, if the water contains chromates or other powerful oxidative impurities, ECP may reach critical values even though O_2 concentrations are as low as 5 ppb.[3] In addition to chemical composition of the coolant, the water flow rate has a significant impact on the corrosion potentials of construction materials as shown in Figure 1.

A possible remedy for the risks caused by the dissolved oxygen and hydrogen peroxide can be suppressed by hydrogen additions to the feed water (hydrogen water chemistry, HWC).[5] HWC was first introduced to protect re-circulating piping welds, but is more recently used to protect internal structures and welds in pressure vessels. The amount of hydrogen needed to decrease the corrosion potential below the threshold potential for SCC is plant- and site-specific depending on the coolant flow rate, construction of the core and dose rate in the down comer.[6]

As a drawback some plants have experienced an increase in the ^{16}N concentration in main steam during the HWC operation, causing elevated dose rates in turbine building. Under normal water chemistry (NWC) operation ^{16}N forms pri-

marily NO_3^-, which remains in water phase, whereas under more reducing conditions NH_3 is formed. NH_3 is volatile, gets easily into the steam phase and is transported into the turbines.[7]

Another side effect of hydrogen water chemistry is a significant increase in shutdown dose rates which has been observed in some boiling water reactors. This phenomena is related to the deposition of the corrosion products on fuel cladding surfaces where they become radioactive. The subsequent dissolution of these activated corrosion products and incorporation into the oxide layers on the out-of-core surfaces of the primary circuit is the major source for activity build-up. If the BWR plant operating under NWC starts to inject hydrogen into the reactor water, the structures of the oxide films will change to adopt into the new environment. This has led to increased activity pickup of the oxide films in such plants. In addition, due to operational realities, hydrogen injection system is not always on-line, which creates a periodic cycling between the reducing (HWC) and oxidising (NWC) conditions, which has shown to further increase ^{60}Co incorporation into the oxides.

2.2 Pressurised water reactors (PWR)

A pressurised water reactor consists of primary and secondary sides. The primary side operates in conditions under which the water passing the reactor core does not boil. This is obtained by maintaining high enough pressure in the primary circuit. The heated water passes through the tubes of the steam generator, transferring its heat to the secondary side to produce steam, which drives the turbines. After the turbines water is condensed and returned by feed water lines back to the steam generator.

Due to the low oxidation rate of the primary loop surfaces and low rate of transport of ions through the existing oxide films, corrosion product concentrations in the coolant during the steady-state operation are low. The solubility studies of different metal oxides have shown that release rates of corrosion products are material specific and vary also as a function of temperature. Therefore, an improved analysis and a narrow range control of primary water chemistry, especially pH_T, in PWRs can be successful in reducing the
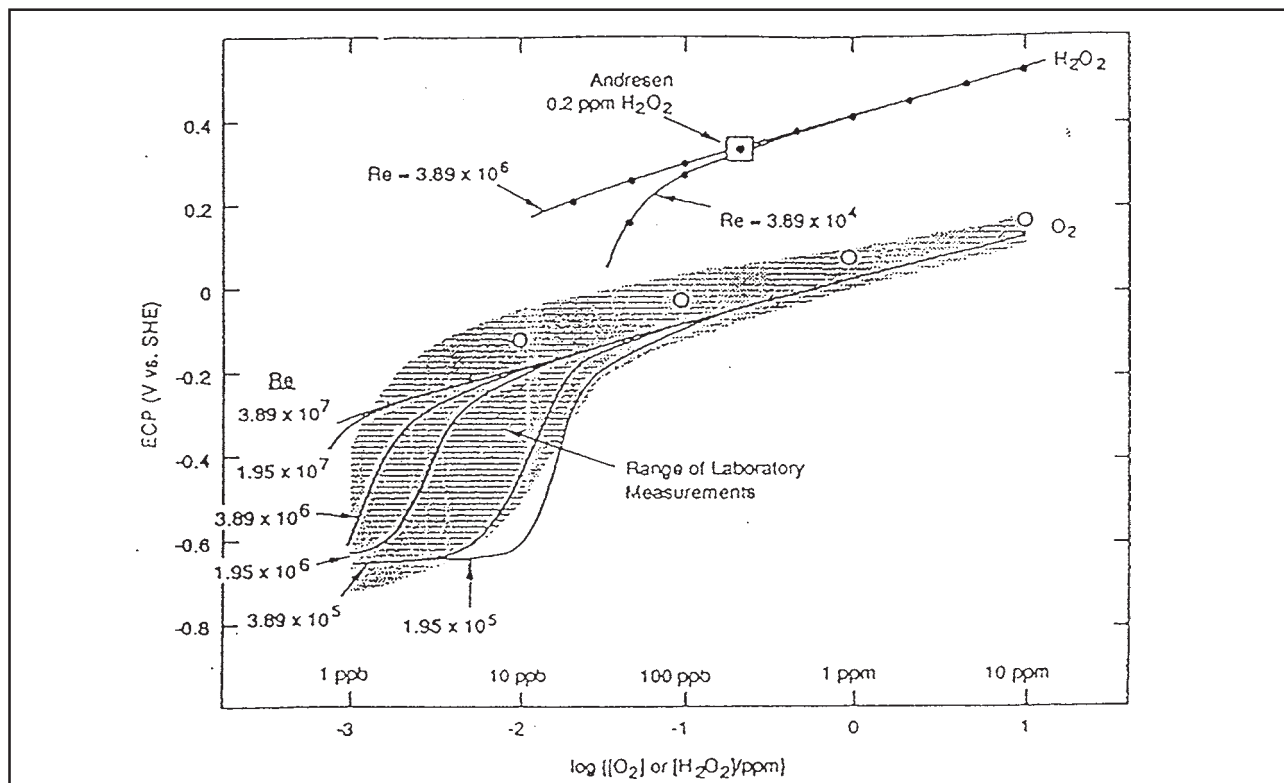

Figure 1. The effect of flow rate (expressed in Reynolds numbers) on the corrosion potential of stainless steel as a function of oxygen and hydrogen peroxide content.[4].

activity build-up.[35,9] The control of pH_T in the PWR primary circuit systems is a rather complicated task. Boric acid is used as a chemical shim to control nuclear reactivity resulting in a need to adjust pH_T by adding lithium or potassium hydroxide to the primary coolant. During the 1980's most plants kept the primary coolant $pH_{300\ °C}$ at 6.9 (called co-ordinated Li-B chemistry), based on the magnetite solubility studies by Sweeton et al, Tremaine et al. [10, 11, 12, 13] These studies showed that 6.9 was the optimum pH_T to prevent deposition of dissolved corrosion products on hot core surfaces due to the positive temperature coefficient of solubility. The oxide examinations in power plants have confirmed that as a result of using this pH_T value, the deposition on hot core surfaces has been reduced.[10] However, more recent solubility studies have shown that the minimum pH_T for a positive temperature coefficient ranges from 6.9 to 7.7. Despite of the large scatter of the data, all the solubility studies indicate that an optimum $pH_{300\ °C}$ is greater than 6.9. Therefore, most of the power plants have started to use so called modified water chemistry, in which a steady-state $pH_{300\ °C}$ of 7.2 is achieved as soon as possible after start-up. This pH_T is kept constant throughout the fuel cycle without exceeding Li concentration of 2.2 $mgkg^{-1}$ to avoid enhanced fuel cladding corrosion.[11,16]

Incorporation of activated corrosion products into the growing oxides can be further decreased by pre-conditioning the replacement parts (like in the primary side channel heads of new steam generators, SG) by using electropolishing or chromium passivation techniques. Both techniques have shown their effectiveness in plant applications (Millstone Point-2 and Doel) by decreasing the surface activities by a factor of two. These two techniques can be easily applied on the new parts to be installed into existing nuclear power plants. However, replacement of large components in operating plants is not done often. Therefore, the optimisation of a plant specific water chemistry may be a more useful way to proceed in operation power plants. One way to optimise water chemistry is to inject a blocking agent into the primary coolant, which decreases incorporation of activity into the oxides. This topic is discussed in more detail in chapters below.

In addition to pH_T control, the PWR primary chemistry guidelines state that the hydrogen content should be kept between 35–55 $mlkg^{-1}$ to minimise the concentration of oxidising species created by radiolysis of water and to reduce the possible traces of oxygen in the make-up water. Because the PWR primary coolants contain high concentrations of dissolved hydrogen, the corrosion potentials of in-core construction materials are likely to be low enough to prevent stress corrosion cracking to occur in thermally sensitised stainless steels observed in BWRs. On the other hand, the use of high hydrogen levels in the primary circuit of PWRs is believed to be a possible cause of cracking of Inconel 600 steam generator tubes (primary water stress corrosion cracking, PWSCC) and other components manufactured from nickel-based alloys. If there is a connection between oxide film properties and PWSCC, then both pH_T and hydrogen concentration in the coolant should also have an impact on PWSCC.[19] The effects of these two chemistry parameters on ion solubilities from the synthetic $Ni_{0.50}Co_{0.05}Fe_{2.45}O_4$, are shown in Figure 2. As the pH_T increases the solubility of iron and cobalt decrease, whereas the solubility of iron and cobalt from the oxide film increases when increasing the hydrogen concentration. The dissolution of the oxide film partly affects the extent of ion transport through the film. Therefore, the dissolution and growth of oxide film has an effect on the vacancy production in the base metal. How this phenomena is related to SCC of construction materials, is discussed below.
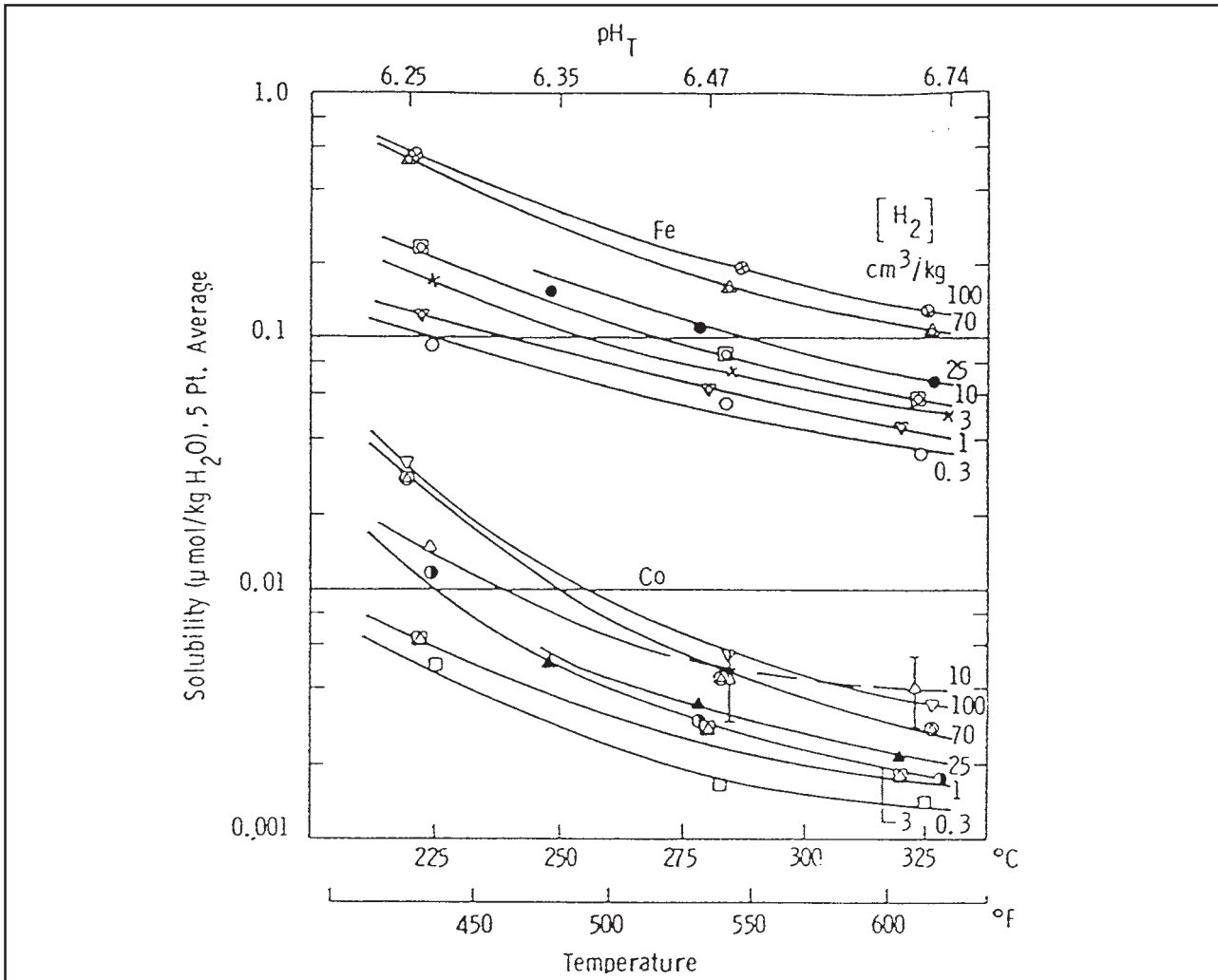
Figure 2. *Average solubility of iron and cobalt from synthetic $Ni_{0.50}Co_{0.05}Fe_{2.45}O_4$ as a function of temperature, pH_T and different hydrogen concentrations.[14]*

3 OXIDE FILMS ON THE CONSTRUCTION MATERIALS IN NUCLEAR POWER PLANTS

The properties of oxide films of construction materials influence the behaviour of the components in operational conditions. The structure of the oxide film determines how different ions are transported into and through the oxides. However, different types of operation environments leads to the formation of different types of oxide film compositions. Therefore, to understand the phenomena occurring on and within the oxide films the most typical oxide film structures are presented in the next chapter.

3.1 Structure of metal oxide films in light water reactors

From a thermodynamic point of view, the stability of an oxide depends on the temperature, pH, oxidising/reducing power of the environment as well as the type and concentration of dissolved ions in the solution. However, an oxide growing on the metal surface cannot be considered as a system in thermodynamic equilibrium. Its properties and composition are to a great extent affected by the kinetic factors determining its growth rate and stationary state thickness. This leads often to the formation of a film in which the composition and stoichiometry changes gradually with distance from the film/environment interface. The oxide films formed at high temperatures in various kinds of environments generally consist of a compact inner layer and of a more porous outer layer. Although this duplex film concept is certainly a simplification, it has proven to be useful in the modelling of the behaviour of the film.

The inner layer consists of fine-grained oxide because it grows in a confined space. The outer layer consists of loosely packed, larger grains because it grows without volume constraint. The boundary between the layers has been found to lie at the position of the original metal surface, which indicates that the inner layer grows at the metal/oxide interface and that the outer layer grows at the oxide/solution interface. It is possible to divide the duplex oxide film further into different sublayers, in which the composition and stoichiometry change gradually with distance.[40,41] The alloying elements are distributed into these two layers differently depending on the primary coolant conditions (pH_T, hydrogen concentration, temperature, etc.) as well as their original concentration in the corroding metal. In addition, the different transport rates of metal ions ($Fe^{2+} > Co^{2+} > Ni^{2+} >> Cr^{3+}$) determine their distribution within the oxides. Slower moving ions tend to be retained in the inner part of the duplex oxide, increasing the chromium content of the inner oxide.

The outer oxide film is partly formed by deposition via the coolant as a result of a high concentration of dissolved species in the bulk solution and—even more likely—a flux of cation species through the oxide film to the solution.[34]. This outermost part of the oxide film has a porous structure, which consists of non-uniform crystallite agglomerates. These crystallites can form as thick layers or exist as single crystallites at scattered sites depending whether mass transport in the system favours re-precipitation. The coolant flow velocity, pH, temperature, water saturation and presence of reducing or oxidising agents influence mainly the properties and behaviour of this outer oxide layer.[37,38,39] Therefore, this part of the oxide film changes most significantly, when the operational environment is changed from oxidising to reducing conditions. Under oxidising conditions, the outer oxide film is either α-Fe_2O_3 (hematite) or γ-Fe_2O_3 (maghemite) independently of the construction material in question, but it strongly depends on the water chemistry. Under reducing conditions, the film changes into magnetite type of spinel. It is possible that below the deposited part of the porous film is formed as a result of breakdown of the inner oxide layer.

On stainless steels and nickel based alloys, the inner, dense part of the duplex oxide film consists of Cr-rich layer, whereas on carbon steels the inner layer is composed of magnetite. This part of the oxide film is often called grown-on oxide, because it grows at the metal/oxide interface. A more comprehensive view can be obtained, if this part of the oxide is divided into two different oxide layers. The composition of the oxide film next to the base metal, does not change due to the changes in operational environments. It is covered by the outer oxide film layers. Therefore, the structure of the film remains similar in both reducing and oxidising conditions. However, it is possible that the composition of the outer part of the inner dense oxide has lower chromium concentration under oxidising environments than under reducing conditions. This is due to higher chromium oxidation rate at higher corrosion potentials.[34,35,36] The formation of the Cr-rich spinels in the dense part of the duplex oxide has been reported to result in a low corrosion rate of stainless steels when compared to the oxidation rate of carbon steels. The overall corrosion rate of stainless steels is likely to be controlled totally by ion transport through this dense oxide layer and is not influenced by fluid flow conditions, by the presence or absence of the outer layer, nor by the saturation degree of the solution. However, the currently used models still need experimental support, specially the preferential paths and driving forces for ion transport through the oxide films, as well as the nature of mobile species/defects.[34,35,36]

3.2 Oxide films on stainless and carbon steels in BWRs

To understand the corrosion processes in boiling water environments, the characteristics of oxide films on AISI 316 SS and AISI 304 SS have been investigated thoroughly. As discussed above, typically these films have a duplex structure. The film composition of the outer part formed under NWC, i.e. under oxidising conditions, differs from that formed under reducing conditions (HWC). Normal water chemistry in BWR conditions leads to the formation of γ-Fe_2O_3, α-Fe_2O_3 and $NiFe_2O_4$ (or $Ni_xFe_{3-x}O_4$) in the outer part of the duplex oxide film on AISI 316 SS, while hydrogen water chemistry results in the formation of Fe_3O_4 and $NiFe_2O_4$ (or $Ni_xFe_{3-x}O_4$). A typical oxide composition in different operating environments is shown in Figure 3. Pores are likely to be present in the outer part of the duplex oxide film, but to a lesser extent in the inner, Cr rich oxide layer.

The inner part of the duplex oxide films on Fe-Cr-Ni alloys may also become partly depleted in chromium if high enough oxygen concentrations exist in the coolant. This behaviour is due to the oxidation of Cr(III) to soluble Cr species.[44]

The composition of the oxide film is rather complicated because, depending on the environment the outer part of the inner, the dense oxide next to the base metal is either $Ni_xFe_yCr_{3-x-y}O_4$ or $Ni_xFe_{3-x}O_4$. It is hypothesised by Asakura et al.[40] that this lowest part of the porous oxide film is formed by the breakdown of the inner layer, which occurs at oxygen concentrations > 100 ppb. This
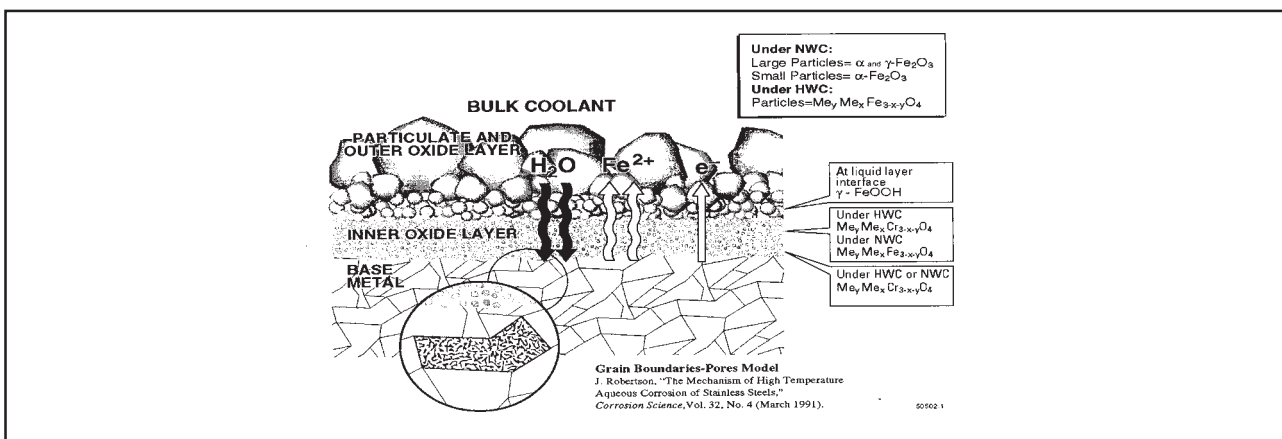

Figure 3. A schematic diagram of the oxide films formed on AISI 316 SS in BWR water under different conditions.[42]

agrees well with the model presented by Hermansson for films grown on stainless steels in BWR coolant under normal water chemistry conditions.[40,41] However, the part of the chromium rich inner oxide, which is next to the base metal, is not affected by the primary coolant chemistry.[8,43]

3.3 Oxide films on alloyed steels and nickel based alloys in PWRs

Corrosion of stainless steel in PWR coolant, i.e. in reducing conditions, results also in the formation of a duplex oxide film on the metal surface if the water above the growing oxide is saturated with corrosion products. On stainless steels the inner oxide layer consists of a chromite ($Ni_xFe_{(1-x)}Cr_2O_4$), usually containing some elemental nickel, while the outer layer is a non-stoichiometric nickel ferrite ($Ni_xFe_{(3-x)}O_4$). On top of this nickel ferrite layer, new single crystals of nickel ferrite can form increasing the total oxide thickness.[45,46,47] Similar duplex oxide films form also on Incoloy 800 (I-800) surfaces. The similarities in the oxide film compositions are not a surprise due to the small differences in base metal compositions.

The oxide films on nickel-based alloys, Inconel 600 (I-600) and Inconel 690 (I-690), are also formed via the same mechanisms as those on stainless steels. The majority of the chromium is retained in the inner oxide film, whereas iron and nickel are mainly present in the outer oxide layer. However, there are some distinct differences in the distribution of ions in the oxides forming on these materials in the high temperature water as discussed below.[48]

The oxides on Inconel alloys can not be solely spinels, because the fixed valences of Ni and Cr (in PWR environments) can only form a spinel of fixed composition $NiCr_2O_4$, whereas the II and III valences of iron allow it to form a continuous series of spinels. Thus, according to the model of Robertson, the inner oxide layer on I-600 may consist of $NiCr_2O_4$ (48%) and NiO (52%), while the outer layer probably consists of NiO with a small quantity of $NiFe_2O_4$.[34] The presence of a substantial proportion of NiO throughout the oxide film allows the oxidation rate to be controlled by the faster growth rate of NiO rather than the slower oxidation rate of Ni,Cr spinel. Therefore, Cr will not lower the non-selective oxidation rate of Ni-Cr alloys until the Cr content increases to 33%, since there will always be some NiO phase present to short circuit the Cr spinel.[34]

The higher Cr content in I-690 when compared to I-600 can lead to a higher concentration of $NiCr_2O_4$ in the inner oxide layer with little NiO incorporation whereas the outer layer should mainly be NiO. The presence of nickel oxide in the inner layer will control the corrosion rate, but the rather low concentration should reduce the oxide growth rate considerably below that of I-600.[34]

However, due to the high hydrogen concentration in the primary circuits of PWRs, NiO is not thermodynamically stable.[46] Schuster et al. have shown that the prevailing oxidation state of nickel was found to be Ni^0, except for a few nanometers at the oxide/solution interface.[49] Furthermore, the water chemistry environments within the cracks and pores differ significantly from the bulk solution conditions, which makes it difficult to estimate the stabilities of the oxides.

4 OXIDE FILMS AND MECHANISMS OF ACTIVITY INCORPORATION AND STRESS CORROSION CRACKING
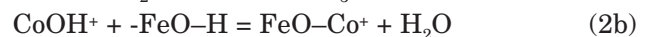
4.1 Activity incorporation

The growth of oxide films is influenced by the extent of saturation of the coolant next to the oxide layer by corrosion products and by the rate of ion transport through the existing oxide. The deposited corrosion products simultaneously in-corporate the activated corrosion products into the oxide films. Additional activity incorporation can occur through deposition of suspended particles on the top of these films. Laboratory tests have shown that ^{60}Co incorporation into the oxide films is directly proportional to the soluble ^{60}Co concentration in the coolant. The accumulation rate into the outer layer increases linearly with the exposure time.

The basic mechanisms of the incorporation of radioactive cobalt into oxide films on iron and nickel-based materials, involve soluble metal ions. The incorporation can basically proceed via at least three different mechanisms:[52]

- surface adsorption/re-crystallisation
- ion-exchange
- direct reaction/crystallisation

The adsorption of radioactive cobalt species on the outer part of the duplex oxide film will result in the formation of nickel ferrite with a basic formula of $(Co_xNi_yFe_{(1-x-y)}O_4)$. The reaction can be initiated by an exchange reaction between a cobalt ion and a surface hydroxyl group of the oxide. Two possible reaction routes have been suggested:

$$Co^{2+} + -FeO\text{-}H = FeO\text{--}Co^+ + H^+ \qquad (1)$$
$$Co^{2+} + 2\,H_2O = CoOH^+ + H_3O^+ \qquad (2a)$$
$$CoOH^+ + \text{-}FeO\text{--}H = FeO\text{--}Co^+ + H_2O \qquad (2b)$$
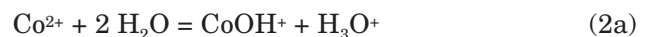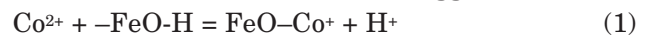
A scheme of the adsorption reaction (1) is shown in Figure 4. The adsorption equilibrium can be described by means of the equation:

$$K = \frac{\left[FeO-Co^+-\right]\cdot\left[H^+\right]}{\left[Co^{2+}\right]\cdot\left[-FeO-H\right]}$$

Figure 4. *Illustration of the adsorption and ion-exchange mechanisms for activity incorporation into oxide films.[52]*

The value of K increases about 600-fold with an increase of temperature from 20 to 285 °C.

It has been suggested that cobalt adsorption takes place only at sites in which the –FeO-H group is available. The rate of Co adsorption is relatively slow compared to the rate of direct reaction/crystallisation. Its rate may increase significantly with increasing the pH and the porosity of the film.[52]
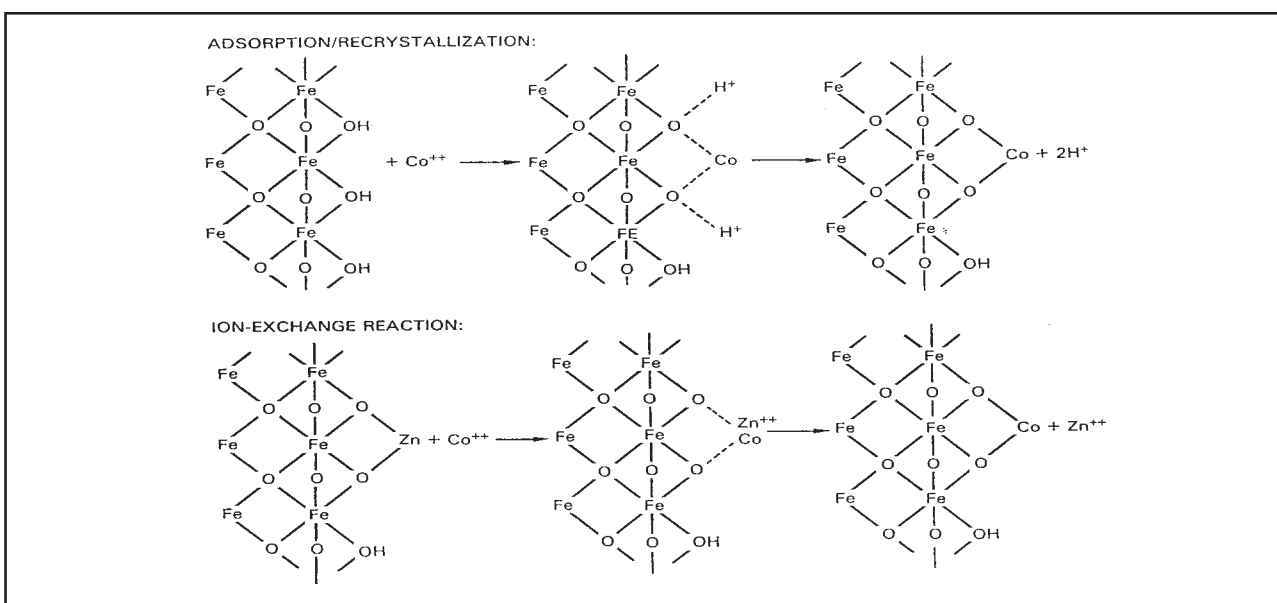
Kelen and Hermansson have discussed the applications of the surface complexation theory with respect to the incorporation of radioactive cobalt into oxide films.[53] The concept of surface complexation refers to the adsorption of dissolved metal species onto the oxide surface as a surface complex, for which surface complex constants can be determined. Accordingly, this approach is analogous to the adsorption mechanism.

The coolant is able to fill the areas between the separate crystals of nickel ferrite on the top of the duplex oxide film. Therefore, a fast solution-diffusion pathway is created for the activated soluble transition metal ions to incorporate into the outer oxide surfaces. If the outer oxide layer contains pores or cracks, the diffusion of metal ions into this oxide layer is much faster than any of the possible solid state diffusion routes. In typical primary coolant environments, a hydrated metal ion has a diffusion coefficient of 10^{-4} cm^{2}s^{-1} as reviewed by Hermansson et al.[41] If there is a sufficient number of the pores and cracks in the outer oxide layer, they provide also an efficient means for the metal ions to be transported transversely throughout the outer nickel ferrite oxide surface. This leads to higher probability for the activated corrosion products to be adsorbed on the surfaces of the porous oxide layer.

The other way for the activated corrosion products to be incorporated into the oxide films is through ion exchange reactions. In this reaction there is a direct exchange between divalent cations in the spinel structure and cobalt ions in the solution. The difference between the ion exchange and adsorption mechanisms is shown in Figure 4. The direct ion exchange requires a high activation energy and therefore it is relatively unlikely in most cases. However, some degree of exchange may be possible if the oxide cracks and/or undergoes morphology transformation resulting in exposure of excessive divalent cations in the oxide to the solution.[52,54]

After diffusing down the pores of the oxide film, the radioactive cobalt species may react either with soluble Ni, Cr and Fe species or with the solid products to form oxide mixtures. This is the third possible mechanism of activity incorporation, that is the direct reaction/crystallisation. It is assumed to proceed at the interface between the dense oxide and the porous part of the oxide film resulting in an oxide structure containing cobalt, possibly according to formula of $Co_xNi_yFe_{(1-x-y)}Cr_2O_4$.[52] The rate of activity incorporation by means of direct reaction/crystallisation is believed to be controlled by the corrosion rate of the base metal, which produces the soluble and solid oxidation products to react with cobalt species. Therefore, incorporation of the radioactive cobalt via this mechanism can be expected to proceed fast on a new surface.[52]

The inner chromite oxide layer of a steady state oxide film does not usually have many pores or cracks. Therefore, the only pathway for the activated or non-activated transition metal ions to be incorporated throughout the oxide is by solid state transport mechanisms. Actually, the same mechanism applies to the parts in the outer oxide layer where no pores or cracks exist. This longitudinal metal ion transport can occur through the grain boundaries or through the crystal lattice of the oxide. The estimated grain-boundary diffusion coefficients are of the order of 10^{-13} cm^{2}s^{-1} compared to 10^{-18} cm^{2}s^{-1} for lattice diffusion.[41]

According to Lister [47], the inner chromium rich oxide film incorporates ^{60}Co strongly, but since it is rather thin, a relatively small amount of activity is involved. The outer ferrite layer is typically thicker, but incorporates less ^{60}Co on a unit mass basis than the inner layer.[47] Similarly, if the outer oxide film is hematite, it will be less protective than the inner parts of the oxide film resulting in increased thickness. However, hematite has no crystal sites for divalent ions and thus activity build-up is lower than expected solely on the basis of the oxide thickness. This suggests that the extent of activity build-up and its distribution in the oxide film is largely determined by the operational environment.

4.2 Oxide films and stress corrosion cracking (SCC)

Stress corrosion cracking (SCC) can be understood as a localised corrosion process, which is caused and/or accelerated by mechanical stresses. Different models developed to explain SCC are, to a great extent, based directly or indirectly on local anodic reaction processes in the crack. Once initiated, the SCC of steels and nickel based alloys has been suggested to proceed in increments (so-called slip-dissolution model).[96] Each increment consists of the following steps at the crack tip:

a) activation, i.e. exposure of new metal surface by mechanical fracture
b) dissolution of the active surface
c) re-passivation

According to the coupled environment fracture model (CEFM) formulated by Macdonald and Urquidi-Macdonald, the crack advance may occur via the slip-dissolution-repassivation mechanism. This model requires charge conservation as a starting point for the calculations.[97] Other competing SCC mechanism models are based on the combination of selective dissolution and vacancy creep, internal oxidation, cleavage and surface-mobility.[98,99,100]

It is assumed in all these models that the anodic and the respective cathodic reactions contributing to crack growth occur partly on or in the oxide films. Thus, the rates of these reactions may control the crack propagation rate, in which case the properties of the oxide films play a crucial role in determining the susceptibility of the material to SCC.

In addition, the surface mobility SCC mechanism [103] and the recently introduced selective dissolution-vacancy creep (SDVC) model for SCC [103,104] include a postulate that the crack growth takes place by capture of vacancies in the metal close to the crack tip. Because the vacancies in the metal lattice can be generated as a result of the dissolution of the metal through the oxide, the crack growth rate may again be controlled by the transport rate of species through the oxide film. Both models require a supply of metal vacancies for the crack growth to occur.

5 NOVEL WATER CHEMISTRIES

5.1 Zinc water chemistry

The first attempts to reduce the exposure were obtained mainly by minimising the time spent by the workers in the radiation fields during the maintenance, inspections and refuelling. The radiation fields were further decreased by optimising start-up, shutdown and steady-state water chemistry conditions as well as applying other remedies such as surface pre-treatments and chemical decontamination of the primary circuit surfaces. The correlation between BWR radiation field build-up and the ionic zinc concentration in the coolant was identified in early 1983. It was observed that the plants, which had brass tubes(source for soluble zinc) in condensers and a powdered resin condensate polishing system, had the lowest activity incorporation into piping surfaces.[59,60] Because of this design combination, these plants were known to have a continuous level of 5 to 15 ppb soluble zinc in the reactor water. The plants using deep bed demineralisers did not have soluble zinc in the coolant, because these demineralisers are superior to the powdered resin filters with respect of the filtration efficiency of ionic impurities. The long flow path through the deep bed demineraliser permits excellent opportunity for ion exchange with the resins resulting usually in removal of over 98% of the ionic species from the coolant, whereas the powered resin filter demineraliser is typically 80% efficient.[61] The plants having stainless steel condensers do not have a natural source of zinc and therefore no soluble zinc in the reactor water. This has been shown to result in higher dose rates on the piping surfaces. The comparison of the various BWR radiation behaviour is shown in Figure 5.

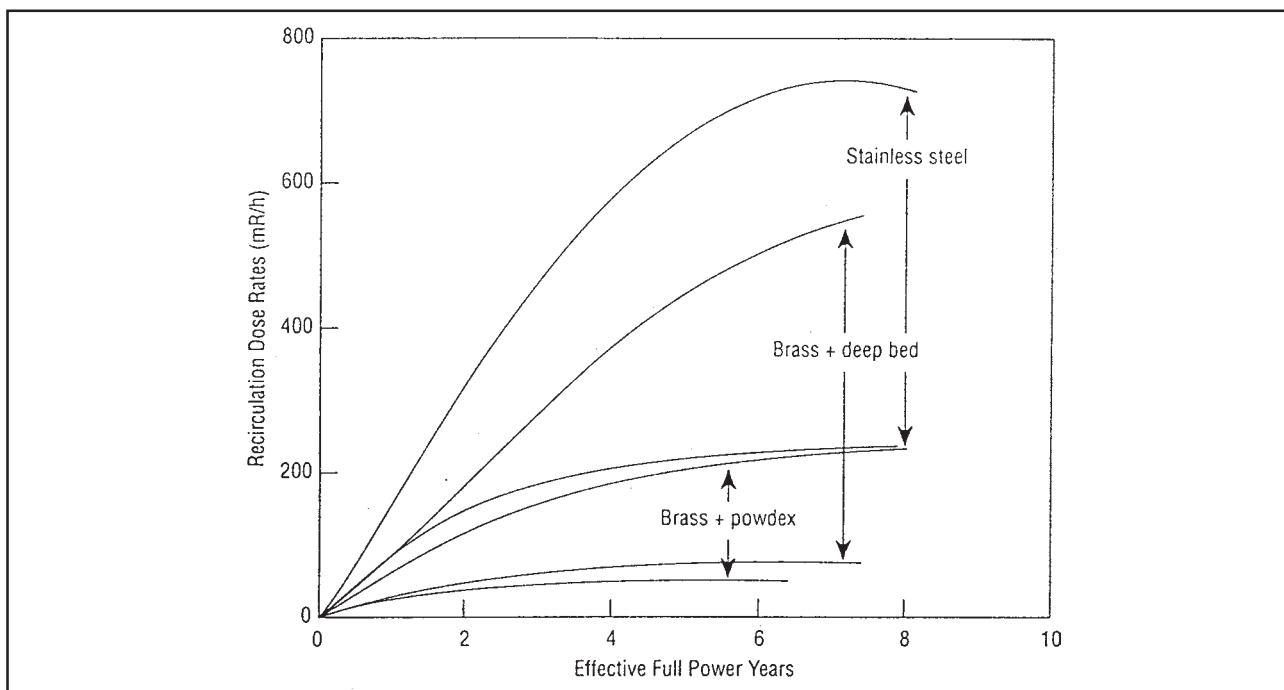Most of the natural zinc plants have nowadays

Figure 5. *BWR radiation behaviour plants when sorted by condenser material and condensate system type.[60]*

either replaced their brass condensers or added deep bed demineralisers to the condensate treatment system to eliminate copper and other harmful ions from the reactor water. In order to maintain low dose rates characteristic to these plants, zinc addition has been implemented. Marble was the first to suggest that zinc addition could be used as a remedy to control activity incorporation into the oxides on the construction materials.[55] It was hypothesised that soluble zinc inhibits the corrosion of stainless steel and thereby reduces the build-up of ^{60}Co into the oxide films. Since then several BWR plants have adapted zinc dosing and have observed clear decrease in activity build-up.

5.1.1 Zinc water chemistry in BWRs

5.1.1.1 Effects of zinc dosing on activity levels in BWRs

Fourteen boiling water reactors were using zinc injections at the end 1994 for the dose rate control.[58] Lin et al.[52] have shown that zinc addition is effective under both NWC and HWC in boiling water reactors, as shown in Figure 6. The
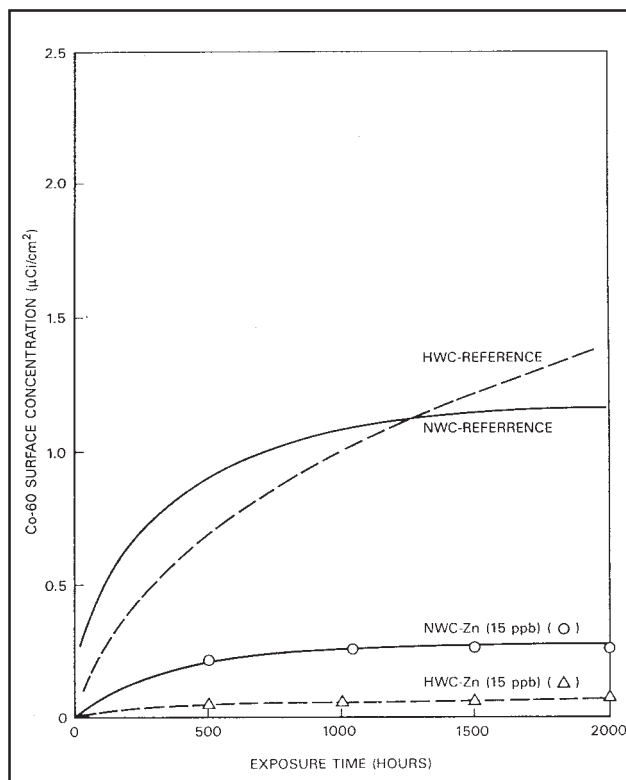

Figure 6. *Effects of zinc ions on ^{60}Co deposition on as-received AISI 304 SS samples under normal and hydrogen water chemistry conditions.[52]*

plant experience has shown that changes in water chemistry (NWC, HWC, NWC, etc.) leads to increased activity levels in the oxide films.[8] However, the expectations for the zinc addition in plants, in which perturbation in the amount of H_2 in the coolant occur, are that the effects of water chemistry changes will be lessened and that the dose rates remain only moderately higher than if the plant is continuously operated under NWC. [61]

The zinc additions can be carried out in different ways. Plants have been using low flow, positive displacement pumps to inject zinc oxide suspension into a re-circulation loop. This system has been further modified by direct zinc injections into the feed water pipe by using higher flow rate injections. The third possibility is to use a passive system without moving parts. In this system, a bed of sintered zinc oxide pellets is contained in a small pressure vessel, through which the primary water is circulated. Sufficient amount of zinc is dissolved from the pellets to maintain the desired concentration of zinc in the reactor water. This technique is attractive, because the operating and maintenance requirements of zinc additions can be minimised. Furthermore, this pellet bed passive system is designed in such a way that it will last at least one full fuel cycle.[60,63]

As discussed later in chapter 5.1.6, the plants which have been dosing natural zinc have experienced one side effect: the activation of ^{64}Zn to form ^{65}Zn, which adds to the inventory of activated corrosion products of the plant. Iron adsorbs zinc and then deposits on the fuel cladding surface, where Zn becomes activated. However, the "natural" zinc plants have had very little problems, because they all have used powdered resin condensate system and thereby have a very little crud input into the reactor feed water. Several plants have nowadays deep bed demineralisers in the condensate system and, as a consequence, have also higher crud input resulting in higher activation of ^{64}Zn.[62] Some plants have started to use Zn, which is depleted in ^{64}Zn to avoid the problem of ^{65}Zn. The content of ^{64}Zn in the depleted zinc oxide (DZO) is reduced from 49% to 1%. However, the cost of DZO is high due to the required processing. Therefore, reduction of iron input in a high crud plants should significantly reduce the cost of using DZO.[60] Moreover, the

impact of DZO will not be seen in the plants, which have earlier had a natural zinc source, for several cycles because of the large natural zinc inventory present in the oxides throughout the reactor surfaces.

Each of the zinc adding plants is, for different reasons, currently using lower zinc concentrations than the recommended 10 ppb as shown in Table I. For the plants using natural zinc oxide the resulting ^{65}Zn has been a concern because of its impact on piping dose rates, radwaste, etc. The plants using DZO are running at reduced zinc concentrations for cost saving reasons.

5.1.1.2 Changes in BWR coolant chemistry during Zn dosing periods

Since soluble zinc is ionic and acts as a weak base, it is to be expected that the addition of zinc will alter both the conductivity and the pH of the reactor water in boiling water reactors. The extent of this effect depends on the concentration of other impurities in the reactor water. If the coolant is acidic without the presence of zinc, then the impact would be to decrease conductivity as a result of a neutralisation reaction. The root cause would be the lower specific ionic conductance of Zn^{2+} when compared to H^+. If the coolant is already basic, the zinc addition would increase both the conductivity and the pH, but only slightly. The plant observations confirm these conclusions. Ho-

Table I. *Typical zinc contents in the reactor water in the plants which are dosing Zn.[61]*

Plant	RxW Zn (ppb)
FitzPatrick	3
Hatch 1	6
Hatch 2	6
Hope Creek	2
Leibstadt	3
Limerick 1	5
Limerick 2	2
Millstone Pt 1	4
Monticello	7
Nine Mile Pt 2	3
Peach Bottom 2	2
Peach Bottom 3	2
Perry	4

wever, small increases in the conductivity and the pH are not considered to have any adverse effects for the BWR.[61,95]

One consequence, which was not anticipated prior to the zinc addition, was the suppression of concentration of the soluble ^{60}Co in the reactor water. This decrease has been found at each BWR, which has started to use zinc after operating for one or more cycles as a non-zinc plant. The comparison of ^{60}Co content in the reactor water before and after Zn addition in four plants is shown in Figure 7.
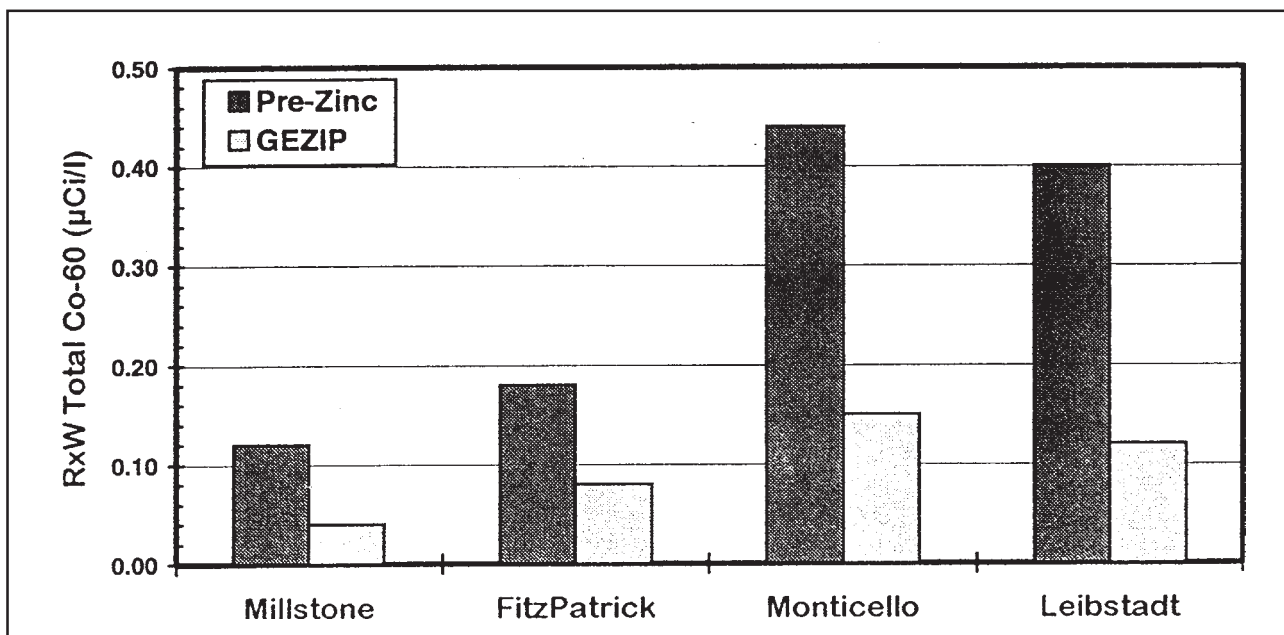

Figure 7. *Reduction of reactor water ^{60}Co as a result of Zn addition.[61]*

Zn is assumed to act in two ways to lower the soluble ^{60}Co concentration in the reactor water. First, it suppresses the corrosion release rates from in-core cobalt alloys, such as Stellite rollers and pins. Second, as zinc is incorporated into the iron based fuel deposits, the release rate of ^{60}Co is lower. This is probably due to the lower solubility of the zinc rich crud, reducing ^{60}Co incorporation into the oxides on primary system piping and components. In addition, due to the lower solubility, the amount of ^{58}Co and ^{60}Co released to the reactor water during a shutdown period is reduced. Therefore, the activity remains within oxides on the in-core materials and in the fuel deposits. As such, part of the activated corrosion products are removed when fuel is replaced. However, the degree of ^{60}Co suppression is a function of the zinc concentration in the reactor water, similarly as the effect of zinc on the reduction in the corrosion rate.[61,62] There are also other explanations: The pH_T may increase significantly close to the fuels cladding surface due to the boiling. This leads to decreased solubility of the fuel crud. Similarly, the pH_T increase would lower the solubility of oxides on in-core Stellite parts.[53,64]

Operational experience has indicated that zinc demand is increased after each refuelling outage as a result of the zinc is dissolved from the oxides during the shutdown period and there are new surfaces inserted during the refuelling.

5.1.2 Zinc water chemistry in PWRs

5.1.2.1 Effects of zinc dosing on activity levels in PWRs

As discussed in the previous chapter, zinc has been used widely in BWRs to obtain lower activity in-corporation into oxides on the primary system surfaces. Several studies have also been carried out in out-of-core loops to evaluate the effect of Zn under typical PWR environments.[18,75,56] The results have shown that dissolved zinc in the range of 10 to 40 ppb reduces the pickup of ^{60}Co by a factor of 8 to 10. Zinc injections have resulted also in thinner oxide films. These studies suggested that zinc addition may be a cost effective method to reduce the rate of activity build-up also on the

primary circuit surfaces in PWRs.[76]

Even though only two operating PWR plants have reported preliminary results from the zinc injection tests, the results so far look rather promising. Investigations at Farley-2 unit have shown that out-of-core exposure rates can be reduced by injecting low concentrations of natural zinc into the primary coolant. The zinc content in the coolant was maintained in a range of 35–45 ppb for approximately nine months. Measured radiation dose rates decreased significantly at steam generator channel heads and at the main coolant piping compared to the cycles without Zn. An encouraging observation was also that ^{65}Zn was less than 10% of the radioisotope mix and only a minor contributor to the increasing dose rates.[57,17]

The second PWR which has performed Zn dosing into the primary coolant, is Biblis NPP in Germany. In Biblis, the dosed Zn concentration was very low (< 5 ppb) and therefore rather small reduction of activity incorporation into the oxide films was observed.[78]

Some controversy exists in the published results. The tests which were carried out at MIT test reactor under PWR conditions using Zn injections showed no beneficial effects on the activity incorporation. In addition, no changes in the amount of deposited corrosion products on the metal surfaces were observed.[78] However, the tests performed at OECD Halden test reactor in typical PWR environments have shown that the activity incorporation during zinc injection periods was lower than in the coolants without Zn addition.

5.1.2.2 Changes in PWR coolant chemistry during Zn dosing periods

The first plant experiments of zinc additions (as zinc acetate) at Farley-2 unit were started in mid June 1994, about six months after the cycle 10 start-up. Zinc was injected for 11 days before it was detected in the primary water.[76] However, during the temperature decreases, the zinc concentration increased even though the Zn injection was stopped. The decrease in the zinc concentration in the coolant was much slower than expected indicating that zinc was being released from the oxide films. After the zinc injection was re-started

and the plant returned to full power operation, the zinc concentrations returned to the nominal level.[77]

The activity of soluble ^{60}Co in the coolant did not change after the Zn injection. A similar trend was also observed at Biblis during the Zn dosing period.[78] A review of the data showed that nearly all of the cobalt activity was in insoluble form in the primary coolant whereas ^{65}Zn activity was predominantly in the soluble form. The calculations showed that some of the ^{65}Zn must have originated from the core crud. This indicates that some of the zinc in the coolant was exchanging with the zinc in the core crud or causing the activated zinc to be released.[76,77]

5.1.3 Effect of zinc on activity incorporation into oxide films

5.1.3.1 Zinc and oxide films under oxidising conditions

The incorporation of zinc can be assumed to depend on the oxide film structures but not on the plant type. Therefore, the effects of zinc dosing discussed in these following chapters are based on the oxidising (BWR, NWC) or reducing (BWR, HWC and PWR) conditions of the primary coolant.

The oxide films on the carbon steel (CS) surfaces under oxidising conditions consist of hematite and spinels. Some laboratory experiments have shown that the greater the content of hematite, the less protective the film is resulting in thicker oxide films. However, hematite has no crystal sites for divalent ions. This explains why Permer et al. results showed that as the outer oxide film consisted mainly of hematite, the amount of Zn and cobalt incorporated into outer oxide layer was low.[66] Thus activity build-up is not solely controlled or explained by the total oxide thickness.

Hanzawa et al. studied the incorporation of cobalt and zinc into the oxide films on carbon steel surfaces using fairly high ionic concentrations (max. Zn = 590 ppb, max. Co =1200 ppb). They found out that the cobalt content in the oxide film increases with increasing Co content in the aqueous phase even though the coolant contained 300 ppb of zinc. They also showed that the increase of Zn in solution decreases the cobalt incorporation into the oxide film. This indicates that zinc ions compete with soluble cobalt ions of the adsorption

sites on the oxide film surface and consequently suppresses the incorporation of cobalt into the oxide films. Another interesting observation was that zinc did not have any effect on the film growth rate on carbon steel in oxidising environments.[72] Similarly, Lister et al. found out that the oxide growth rate of the CS sample exposed to zinc containing coolant did not differ significantly from the growth rate of the oxide on the carbon steel sample which was grown without Zn.[46]

When effects of zinc dosing on behaviour of stainless steel samples were studied, the observations of the oxide growth rates and ion release rates from SS oxide films turned out be totally different. Lister et al. has shown that dissolved Zn has a profound effect on the release rates of corrosion products from stainless steel even in NWC conditions. His experiments demonstrated that addition of Zn resulted in thinner and more protective oxide films. In addition, the release rate of cobalt from the base metal and oxide was far lower than that observed in the normal BWR conditions. This indicates that zinc somehow decreased the transport rate of cobalt ions through the oxide.[46]

Lin et al. verified in their zinc injections tests, (10 ppb of Zn) that ^{60}Co incorporation into the oxide film on both AISI 304 SS and AISI 316 SS was low as shown in Figure 6.[52] They was observed also that the higher Zn concentration in the coolant, the less activity is incorporated into the oxide, but addition of Zn did not replace the cobalt from the oxide as shown in Figure 8. Both Co and Zn had highest concentrations on the oxide surface. However, some tests showed that the cobalt accumulation rate into the inner layer decreased by zinc addition even though cobalt was dosed into the coolant continuously. Permer et al. have also reported that Zn had a maximum concentration in these parts of the oxide in which chromium concentration was also highest.[46,66]

These results seem to indicate that zinc addition reduces significantly the ^{60}Co incorporation into the oxide films on stainless steels as well as reduces the ion transport through the oxide leading to thinner oxide layers. However, the zinc dosing seems to have rather small impact on the behaviour of oxide films on carbon steels under oxidising conditions.

5.1.3.2 Zinc and oxide films under reducing conditions

An important aspect of surface oxide films formed under oxidising and reducing conditions is their spinel structure and distribution of metal cations therein, because activity incorporation into the oxide films can not be only related to film thickness but is also strongly affected by film characteristics and composition.

As shown in the previous chapter, Zn addition did not have a significant effect on oxide growth rate on carbon steel surfaces in oxidising conditions. Similarly Allsop et al.[73] have shown that those carbon steel coupons, which were exposed to Zinc containing coolant in reducing conditions had only slightly thinner oxide films on the surface (2.7 μm with zinc: 3.7 μm without Zn). During these tests in reducing environments it was shown
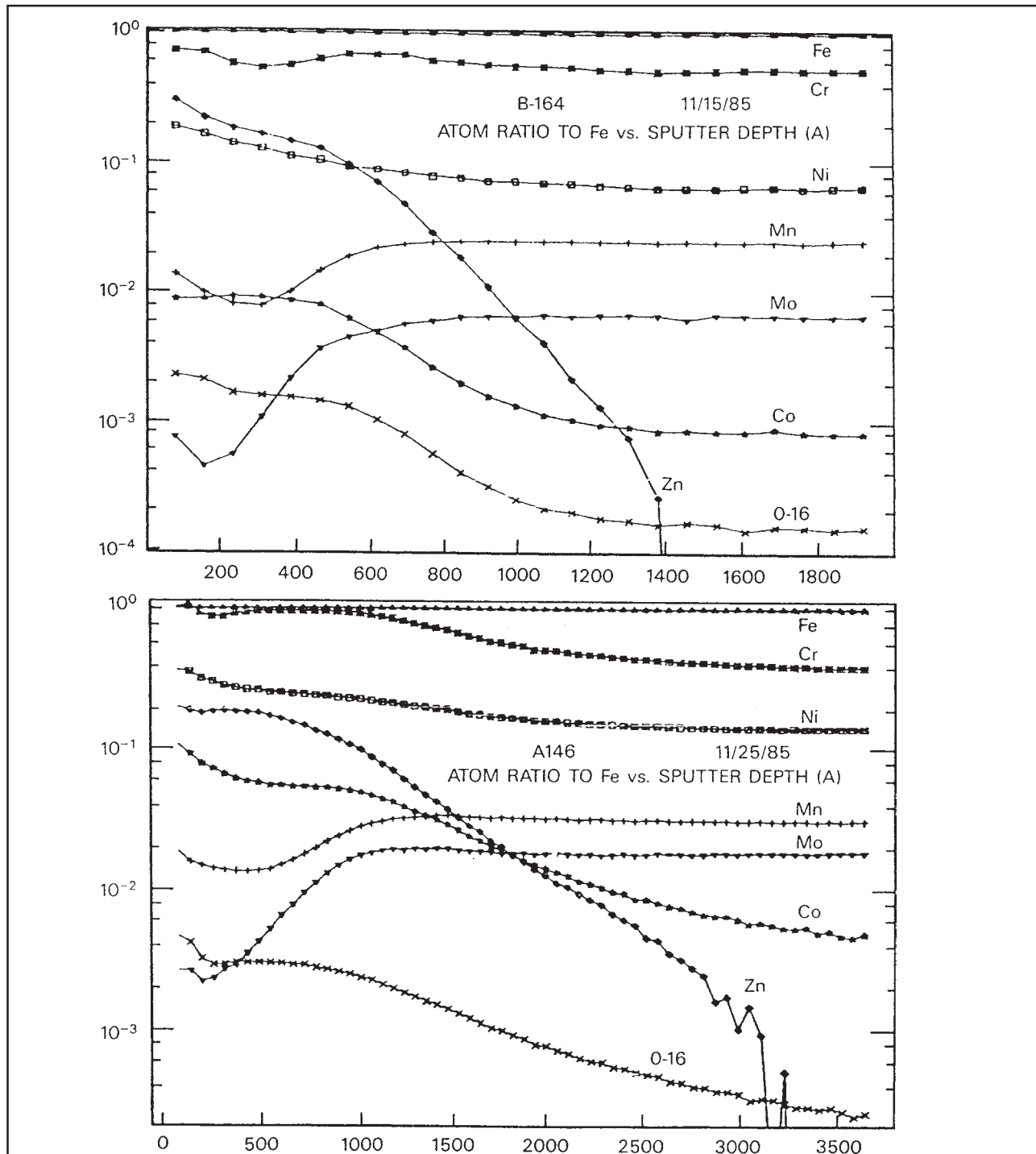

Figure 8. *Elemental depth profiles in oxide films (AISI 304 SS, AR and AISI 316 SS,AR) exposed to NWC-Zn(15 ppb) and NWC-without Zn conditions.[52]*

that zinc seemed to have very little effect on activity in-corporation into the oxide films on the CS coupons whereas a significant difference was observed in stainless steel coupons. Based on these results it is clear that also in reducing environments Zn has smaller effect on oxidation behaviour of carbon steel when compared to the results obtained for stainless steel.[8,73,74]

Riess et al. [80] studied the influence of zinc on the oxide films and activity incorporation of the sample which had been exposed prior the tests in the steam generator channel head of a PWR over two years. They reported that the oxides on stainless steel specimens which were exposed to zinc environments incorporated zinc up to 16%. These results also showed that after the Zn injection ca. 50% lower γ-activity was measured on the samples due to the activity release into the coolant.[80] Therefore Riess et al. concluded that zinc is very efficient in displacing ^{60}Co from the contaminated system surfaces. The initial rate of displacement of cobalt and other elements from existing oxide is apparently very high.[80] The spinel composition on the specimens ranged from $(FeNiZn)Cr_2O_4$ to $(FeNiZn)FeCrO_4$. In addition, some of the particles on the coupon surfaces were analysed and they corresponded roughly to the spinel $Ni_{0.5}Zn_{0.5}Fe_2O_4$.[80] However, Fe,Ni-spinels were detected only in isolated cases, which is not typical for oxides grown in high temperature water under PWR conditions. This could indicate that for some reason some of the outermost deposited layer had been removed during the zinc injection periods. The fact that the oxide thickness of SS decreased during the exposure to the zinc containing coolant was also partly supported by Riess et al.

The studies carried out at OECD Halden Reactor Project have shown that zinc injection to the primary coolants results in thinner oxide layers on new metal surfaces (SS, I-600, I-690, Incoloy 800) with low visible porosity. In addition Zn injection hinders the incorporation of activity into already existing oxides.[82,83,84,85] During the zinc injection tests, activity pickup of the oxide films was low in all the studied samples. In addition, the oxides did not grow in thickness, because the corrosion product deposition from the solution was minimal. The lack of thick deposited oxide layer partly explained also the observed reduction in activity incorporation during Zn in-

jection periods.[82,83,84,85] The deposition rates of corrosion products on primary circuit surfaces were low, since their concentrations in the coolant decreased due to the restricted diffusion of ions through the oxide films. The effect of Zn on the activity build-up is partly due to the fact that a smaller amount of corrosion products are released to the coolant, i.e. less corrosion products, which can become active and be redeposited on the tubing.[18,20] However, the tests at Halden have shown that the rate of activity build-up on out-of-core surfaces can be reduced only with continuous zinc injection. Once the injection of zinc into the coolant was stopped, the activity incorporation into the stainless steel started to increase.[84,85]

In some tests zinc concentrations have been highest on the oxide surface and decreased rapidly deeper in the oxide. The zinc concentration throughout the oxide film appeared to increase with exposure time, both in terms of the maximum surface concentration and the depth of the zinc enriched layer. In this process, time appeared to be more determining than the zinc concentration in the coolant, probably due to complex kinetics associated with combined diffusion and ion exchange reactions. In one of the test performed in Halden, the surface enrichment of Zn was related to high Cr concentration on the outer oxide film.[85] During tests done by Korb et al., it was observed that ZnO was formed on the oxide surface, due to the very high soluble zinc concentrations in the coolant (up to 281 ppb).[81] These findings are supported by Beverskog et al. who reported that the solubility limit of ZnO to be roughly 60 ppb.[71,86] In some cases the highest zinc concentration have been measured between the inner and outer oxide films, where also the highest Cr concentration existed.[66,85] These results seem to indicate that zinc has a fairly high affinity for Cr rich oxide layers.

Some results show that the decrease in ^{60}Co deposition caused by zinc seems to be greater than the decrease in the film thickness, indicating that Zn may modify the propensity of the oxide to incorporate ^{60}Co.[18,68] Similar results were obtained also in Halden. Those test showed that even though the oxide thickness did not change on the studied coupons, the total amount of incorporated activity remained lower than during the periods without Zn.[85]

Table II. Distribution of ions in tetrahedral and octahedral positions in normal and inverse spinels.

	Occupied close-packed positions	Occupied tetrahedral positions	Occupied octahedral positions
Normal spinel AB_2O_4	32 O^{2-}	8 A^{2+} ions	16 B^{3+} ions
Inverse spinel $B(AB)O_4$	32 O^{2-}	8 B^{3+} ions	8 A^{2+} and 8 B^{3+} ions

5.1.4 Correlation between role of Zn and oxide structure

The oxides formed on the primary circuit construction materials in light water reactors are usually spinels. On carbon steel, the oxide can be either a magnetite or maghemite spinel depending on the reducing or oxidising power of the coolant. On alloyed steels, the alloying elements are incorporated in the growing spinel oxides more or less in the proportion to their concentration in the base metal. The structure of spinel oxides, the cation distribution in them as well as defects in oxides are presented in this chapter. Moreover, the possible mechanisms of the zinc cation incorporation into the oxide films are discussed on the basis of these concepts.

5.1.4 Structure of spinel oxides

Bulk oxides are crystalline compounds, which consists of ions packed regularly in a three dimensional arrangement. For any points in the pattern, it is possible to find other points possessing exactly the same surroundings. Such points define a regular lattice. One lattice point can be reached from another point by taking a suitable number of steps along each of three directions. This small volume of atoms/ions is called a unit cell. The whole lattice can be built up by these unit cells.[21]

The most efficient packing of uniform spheres (ion/atom) forms a close-packed layer of spheres.
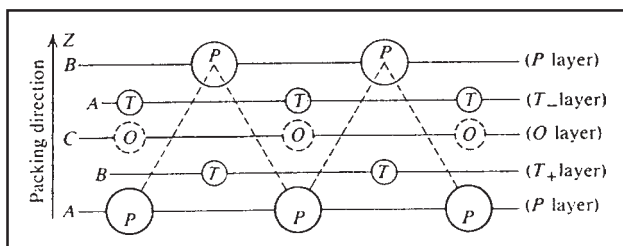

Figure 9. Construction of the basic close-packed unit (two packing layers for any closed-packed structure). P = oxygen ion, O = octahedral site, T = tetrahedral site, A,B,C, the three relative packing positions.[22]

Spinel structures are based on close-packed arrays of oxygen ions, which are on a face-centred cubic lattice. Each unit cell of a spinel lattice contains eight (8) formula units of AB_2O_4. This means that each unit cell contains 32 O^{2-} ions. Because the spinel must be electrically neutral, each unit cell must contain 64 positive charges. In the face-centered cubic close-packing, each sphere is surrounded by twelve nearest neighbours. The volume of the structure containing n spheres with the radius r is $5.66*r^3*n$. If there are n spheres in the system, there are $2*n$ tetrahedral sites and n octahedral sites. This means that in a unit cell containing 32 O^{2-} ions, there are 64 tetrahedral sites and 32 octahedral sites.[22] The positions of the sites lie as shown in Figure 9.

5.1.4.2 Classification of spinel oxides

Spinels can be classified as normal, inverse and intermediate, depending on the location of A^{2+} and B^{3+} ions in the tetrahedral and octahedral positions. Table II shows how the lattice sites are occupied in normal and inverse spinel:

Higher valency cations tend to prefer the octahedral holes.[23] When all the eight A^{2+} cations exist in the tetrahedral positions and all the sixteen B^{3+} cations in the octahedral positions, a normal spinel structure prevails. In an inverse spinel eight higher valency B^{3+} ions are located in the tetrahedral positions, and the remaining eight B^{3+} ions and the eight A^{2+} ions with a lower charge occupy the sixteen octahedral positions in a statistically disordered manner.

The normal and inverse spinels correspond to the extreme values of distribution of B^{3+} ions between tetrahedral and octahedral sites. In intermediate spinels the A^{2+} and B^{3+} cations are arranged in a disordered manner both in tetrahedral and octahedral positions.[23]

A^{2+} and B^{3+} ions can be arranged in three different ways to obtain an electrically neutral

Table III. *Examples of typical normal and inverse spinels. The results are based on experimental results, not on predictions by the crystal field theory.[24,25,69]*

Normal spinel					
Mineral name		Tetrahedral site	Octahedral site	Close-packed	Empty tetrahedral/octahedral sites in a unit cell
Franklinite	$ZnFe_2O_4$	8 * Zn^{2+}	8 * $(Fe^{3+})_2$	8 * $[O^{2-}]_4$	56/16
Danathite	$ZnCr_2O_4$	8 * Zn^{2+}	8 * $(Cr^{3+})_2$	8 * $[O^{2-}]_4$	56/16
	$CoCr_2O_4$	8 * Co^{2+}	8 * $(Cr^{3+})_2$	8 * $[O^{2-}]_4$	56/16
	$NiCr_2O_4$	8 * Ni^{2+}	8 * $(Cr^{3+})_2$	8 * $[O^{2-}]_4$	56/16
Chromite	$FeCr_2O_4$	8 * Fe^{2+}	8 * $(Cr^{3+})_2$	8 * $[O^{2-}]_4$	56/16
	$MgCr_2O_4$	8 * Mg^{2+}	8 * $(Cr^{3+})_2$	8 * $[O^{2-}]_4$	56/16
	$MnCr_2O_4$	8 * Mn^{2+}	8 * $(Cr^{3+})_2$	8 * $[O^{2-}]_4$	56/16
Inverse spinel					
Mineral name		Tetrahedral site	Octahedral site	Close-packed	Empty tetrahedral/octahedral sites in a unit cell
CoFerrite	$CoFe_2O_4$	8 * Fe^{3+}	8 * $(Co^{2+} + Fe^{3+})$	8 * $[O^{2-}]_4$	56/16
Trevorite	$NiFe_2O_4$	8 * Fe^{3+}	8 * $(Ni^{2+} + Fe^{3+})$	8 * $[O^{2-}]_4$	56/16
Magnetite	Fe_3O_4	8 * Fe^{3+}	8 * $(Fe^{2+} + Fe^{3+})$	8 * $[O^{2-}]_4$	56/16
	$MgFe_2O_4$	8 * Fe^{3+}	8 * $(Mg^{2+} + Fe^{3+})$	8 * $[O^{2-}]_4$	56/16
Jacobsite	$MnFe_2O_4$	8 * Fe^{3+}	8 * $(Mn^{2+} + Fe^{3+})$	8 * $[O^{2-}]_4$	56/16

spinel structure:

(i) $[A^{2+}(B^{3+})_2]_8$ 2:3 spinel

(ii) $[A^{4+}(B^{2+})_2]_8$ 4:2 spinel

(iii) $[A^{6+}(B^{+})_2]_8$

4:2 spinels are found in an inverse structure only, one example being $[Ti^{4+}(Zn^{2+})_2]_8$. Spinels of the form 2:3 are found both in the normal and inverse class. Some examples of these structures are shown in Table III.

Several factors, such as hydration energy and electrostatic forces between different ions contribute to the stability of an ion in an octahedral or tetrahedral site.[26] However, an estimation of the crystal field stabilisation energy of a cation alone gives a reliable indication whether the ion will occupy an octahedral or tetrahedral site determining which type of spinel structure is favoured.

5.1.4.3 Metal ion distribution in the spinels according to crystal field theory

The structure of spinels can be predicted in terms of the valence bond [28] and the molecular orbital theories [28], but they are rather complicated to be applied on spinels. An other possibility to estimate spinel structures and how different ions af-

fect the stabilities of different structures, is to use crystal or ligand field theory. In spite of the approximations, these theories yield quantitative results which are more in accordance with experimental values than are the results of calculations based on valence and molecular orbital theories. The approximations used in crystal field theory, are also included to the ligand field theory, which differs from crystal field theory only in two ways. In the ligand field theory, the transition metal ion is described to be surrounded by ligands which are either negative ions or highly polar molecules; at a greater distance are the ions of opposite sign to that of the transition metal complex ion. The ligand field also persists so long as the complex persist and is therefore present not only when the complex is crystalline, but also when it is a vapour, a melt or in solution. In the following chapters, the stability of octahedral and tetrahedral complexes is discussed on the basis of crystal field theory.

In an oxide consisting of a close-packed structure of negative ions (like O^{2-}), the transition metal ions are in the sites between them. Their *d* orbitals are exposed to the field between metal nucleus and the negative charge of the surrounding ions. This field is known as the crystal field.

The crystal field theory assumes that the interaction between the transition metal ion and surrounding oxygen ions is purely electrostatic and no covalency is included (no combination of orbitals).[27] The field has also a definite symmetry and produces similar effects on all of the *d* orbitals.

The five *d* orbitals (of the transition metals from Cr to Zn) in the isolated, gaseous metal ion are degenerate (not split) as shown in Figure 10b. If a spherically symmetric field of negative charges is placed around the transition metal ion, the energies of all five orbitals will be raised as a result of the repulsion between the negative oxygen ion and the negative electrons in the orbitals. The five *d* orbitals remain still degenerate. If the field results from the influence of the real crystal system, the symmetry must be less than spherical because of the finite number of oxygen ions involved. This leads to splitting of the energy levels of *d* orbitals, which, on the other hand, also stabilises the system. The magnitude of splitting varies from 10^{-6} eV to 5 eV depending on the anions causing the splitting. In the crystal field approach, the used splitting energy is denoted with 10 Dq by definition. In ligand field theory Δ_o is used usually to describe the same parameter. The five d orbitals are split to the e_g and t_{2g} orbitals as shown in Figure 10a.

In order to understand the interactions that are responsible for crystal field effects, it is necessary to understand the geometrical relationships of *d* orbitals. In the case of six O^{2-} ions approaching a transition metal ion to form an octahedral compound, the six oxygen anions enter along the axes of the co-ordinate system, i.e. from the directions z, –z, x, –x, y and –y as shown in Figure 11.[28] Under these conditions, the anions will interact strongly with two e_g orbitals (shaded) lying in the x, y z axis. The remaining three t_{2g} orbitals (unshaded) will be interacted to a lesser extent, because they are directed between the approaching anions as shown in Figure 11.

The energy of the orbitals may be raised by the repulsion of the oxygen anions. However, by rearranging the O^{2-} ions from a hypothetical spherical field to an octahedral field does not alter the average energy of the set of *d* orbitals. Hence to maintain the barycenter it is necessary for the 2 e_g orbitals to be repelled by an energy of 6 Dq to balance the stabilisation of the 3 t_{2g} orbitals to the extent of 4 Dq as shown in Figure 11. This constancy of the barycenter of the d orbitals is linked to the conservation of the orbital energy $(2*6 Dq + 3*(-4 Dq) = 0)$. So the energy of the t_{2g} level relative to the barycenter of unperturbed *d* orbitals is –4 Dq which is the *crystal field stabilisation energy* (CFSE) in the case of d^1. For d^3 (three electrons in d orbitals) the CFSE is –12 Dq. In these configurations, the electrons remain unpaired and enter different degenerate orbitals. However, the fourth electron can not be placed in to the t_{2g} levels, without electron pairing. In the weak field limit (low CFSE) the splitting of the orbitals (10 Dq) is small with respect to the energy necessary to cause electron pairing in a single orbital and the fourth electron to enter one of the e_g levels (leading to a high spin complex). The oxide ions in spinels provide a moderately weak crystalline field and therefore the weak field situ-
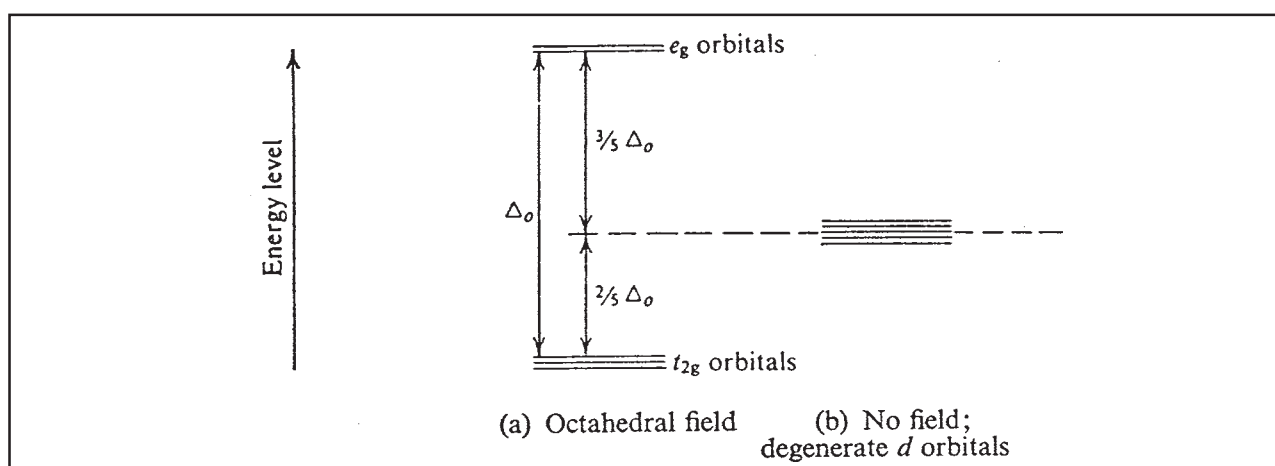

Figure 10. *Diagrammatic presentation of the splitting of d orbitals caused by electrostatic octahedral field as well as no field situation.[27]*

***Table IV.** Crystal field effects for weak octahedral and tetrahedral fields.*

d^n	Octahedral field			Tetrahedral field	
	Configuration	Unpaired electrons	CFSE	Configuration	CFSE
d^1	t^1_{2g}	1	–4 Dq	e^1	–6 Dq
d^2	t^2_{2g}	2	–8 Dq	e^2	–12 Dq
d^3	t^3_{2g}	3	–12 Dq	$e^2t^1_2$	–8 Dq
d^4	$t^3_{2g}e^1_g$	4	–6 Dq	$e^2t^2_2$	–4 Dq
d^5	$t^3_{2g}e^2_g$	5	0	$e^2t^3_2$	0
d^6	$t^4_{2g}e^2_g$	4	–4 Dq	$e^3t^3_2$	–6 Dq
d^7	$t^5_{2g}e^2_g$	3	–8 Dq	$e^4t^3_2$	–12 Dq
d^8	$t^6_{2g}e^2_g$	2	–12Dq	$e^4t^4_2$	–8 Dq
d^9	$t^6_{2g}e^3_g$	1	–6 Dq	$e^4t^5_2$	–4 Dq
d^{10}	$t^6_{2g}e^4_g$	0	0	$e^4t^6_2$	0

ations are only considered in this report. The net CFSE energy is then:

$$CFSE = (3*-4\ Dq) + (1*6\ Dq) = -6\ Dq \qquad (t^3_{2g}e^1_g)$$

The addition of a fifth electron results in a half filled *d* orbitals and the CFSE is zero. The presence of two electrons in the unfavourable e_g level exactly balances the stabilisation resulting from the three electrons in the t_{2g} level. The remaining electrons are placed to the orbitals in the similar way and the resulting CFSE are listed in Table IV, together with the number of unpaired electrons expected for each configuration.

Two of the most common geometries for a 4 co-ordinate compound are the tetrahedral and square planar arrangements. The square planar geometry is a special case and not discussed in this review. Energy level scheme for tetrahedral sym-metry is qualitatively similar to that for cubic system, only the splitting (10 Dq) is half as large. The *d* orbitals and their splitting in tetrahedral complexes are shown in Figure 12.

In Figure 12, eight oxygen anions are approaching the central transition metal ion. If four ligands are removed from the alternate corners of the cube as shown in Figure 12, the remaining oxygen anions form a tetrahedron around the metal. In this arrangement the O^{2-} ions do not directly approach any of the metal *d* orbitals, but come closer to the t_2 orbitals directed to the edges of the cube than to the e levels directed to the centres of the faces of the cube. Hence the t_2 levels are raised in energy and the e levels stabilised. Furthermore, since the barycenter rule holds, the three t_2 levels are raised by 4 Dq and the two e levels lowered by 6 Dq from the barycenter. The

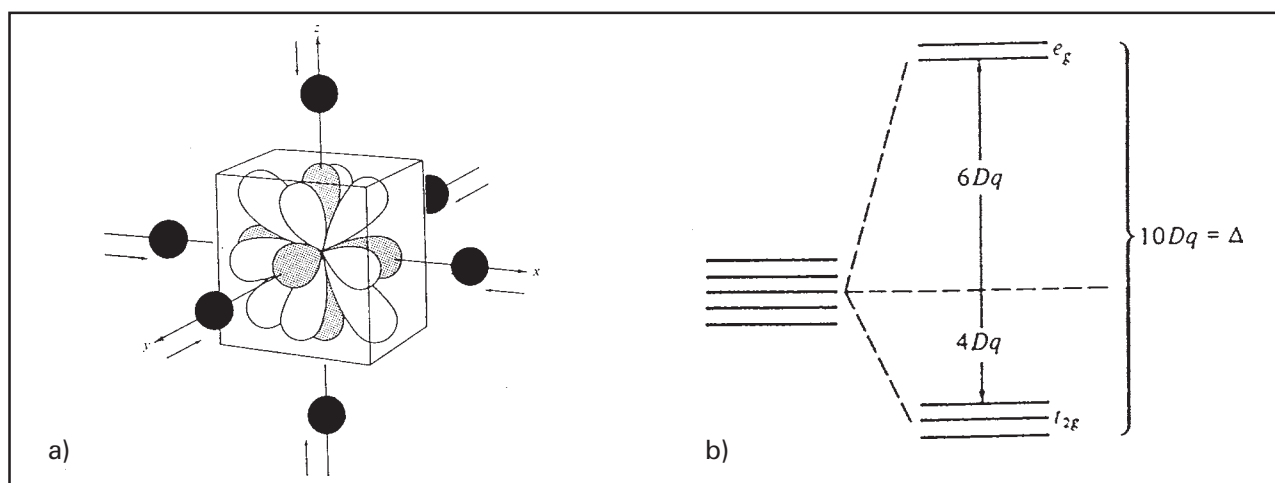
***Figure 11.** Complete set of* d *orbitals in an octahedral field. The e_g orbitals are shaded and the t_{2g} orbitals are unshaded (a). Splitting of the degeneracy of the five* d *orbitals by an octahedral field (b).[28]*

energy levels for the tetrahedral symmetry are exactly the inverse of that for octahedral symmetry. The electron pairing energy is larger than 10 Dq and the electrons enter the five orbitals remaining unpaired until the sixth electron forces pairing. The d^4 case results in an $e^2t^2_2$ configuration with crystal field stabilisation of -4 Dq:

CFSE = (2 * $-$ 6 Dq) + (2 * 4 Dq) = -4 Dq

The number of the unpaired electrons, the configurations and CFSEs are given in Table IV. Since the absolute value of 10 Dq (in $kJmol^{-1}$) is less in tetrahedral complexes than in octahedral ones (because of the indirect effect of the O^{2-} ions and their smaller number), the total crystal field stabilisation is much less important than with octahedral complexes. There are several factors affecting the extent of splitting of the d orbitals. Some values for 10 Dq of aqua complexes of the metal ions of the first transition metal series are listed in Table V.

Some trends in the table become apparent. The ionic charge on the metal ion has a direct effect upon the magnitude of Dq. This is expected, since the increased charge of the metal ion will attract the O^{2-} ions more closely, hence they will have a greater effect on perturbing the metal d orbitals. Secondly, the splitting in an octahedral field is more than twice as strong as for a tetrahedral field from the same metal ion:

10 Dq_{td} = 4/9 * 10 Dq_{oh}

in which 4/9 is based on the square of the ligand interactions ($4^2/6^2$).

There are several factors that influence the adoption of tetrahedral or octahedral co-ordination, and occasionally the balance between opposing factors is a delicate one. From a purely electrostatic viewpoint, octahedral co-ordination is favoured because six ligands are approaching instead of four (O^{2-}). On the other hand, if the ligands are bulky then the ligand-ligand interaction may cause some opposing effects.

Tetrahedral complexes are always in the high spin. As a result, the maximum CFSE can be 12 Dq which converted to octahedral field equivalents, is only 5 Dq (12 Dq*4/9). Therefore, when comparing a given ion in a tetrahedral field with the same ion in an equivalent octahedral site, the ion is always at least as stable in the octahedral hole, usually more so. The difference in energy which always favours the octahedral case, is termed octahedral site stabilisation energy (OSSE), since the term was originally applied to cationic preference for octahedral holes in anionic lattices. Some estimates of OSSE in $kJmol^{-1}$ are shown in Table VI.

For some configurations, such as d^1, d^2, d^5 (Zn^{2+}), d^6, d^7 and d^{10} the advantage of the octahedral arrangement in spinels is little or nothing. Others, such as d^3 (Cr^{3+}) and d^8 (Ni^{2+}), are strongly favoured to be octahedral as shown in Table VI.

Fe^{3+} in trevorite ($NiFe_2O_4$), is located both in tetrahedral and octahedral sites and Ni^{2+} in octahedral sites as shown in Table III. For the d^5 Fe^{3+} ion the CFSE is zero for both tetra and octahedral sites, but the d^8 Ni^{2+} ion has an OSSE of 8.45 Dq (Table VI) or approximately 96 $kJmol^{-1}$ (Table V). This CSFE advantage for Ni^{2+} ion in the octahedral holes is sufficient to invert the structure. Similarly also in magnetite, Fe_3O_4, the d^6 Fe^{2+} ion
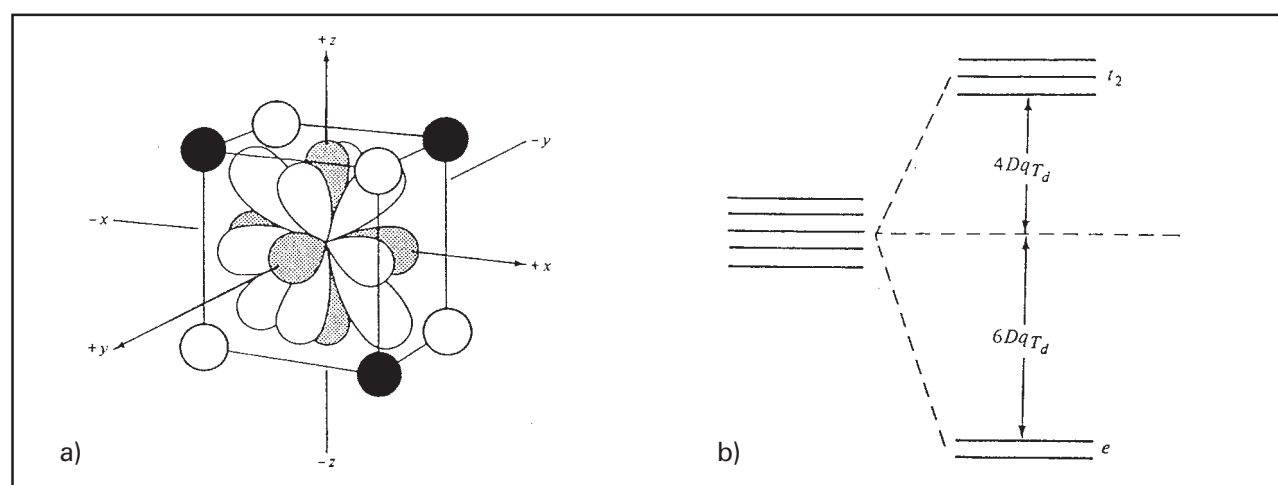

Figure 12. *Complete set of* d *orbitals in a tetrahedral field. The e_g orbitals are shaded and the t_{2g} orbitals are unshaded (a). Splitting of the degeneracy of the five* d *orbitals by an tetrahedral field (b).[28]*

Table V. *Crystal field theory data for metal ions of the first transition metal series in aqua complexes.[28]*

Number of d electrons	Ion	Free ion ground state	Octahedral field ground state	Tetrahedral field ground state	Dq (cm^{-1})	Dq (cm^{-1})	Stabilization (kJ mol^{-1})		Oct. site preference energy (kJ mol^{-1})
					oct.	tetr.	oct.	tetr.	
1	Ti^{+3}	^2D	t^1_{2g}	e^1	2030	900	96.6	64.4	32.3
2	V^{+3}	^3F	t^2_{2g}	e^2	1800	840	174.5	120.0	54.5
3	V^{+2}	^4F	t^3_{2g}	$e^2t^1_2$	1180	520	168.0	36.4	131.6
	Cr^{+3}	^4F	t^3_{2g}	$e^2t^1_2$	1760	780	250.8	55.6	195.2
4	Cr^{+2}	^5D	$t^3_{2g}e^1_g$	$e^2t^2_2$	1400	620	100.3	29.3	71.0
	Mn^{+3}	^5D	$t^3_{2g}e^1_g$	$e^2t^2_2$	2100	930	150.1	44.3	105.8
5	Mn^{+2}	^6S	$t^3_{2g}e^2_g$	$e^2t^3_2$	750	330	0	0	0
	Fe^{+3}	^6S	$t^3_{2g}e^2_g$	$e^2t^3_2$	1400	620	0	0	0
6	Fe^{+2}	^5D	$t^4_{2g}e^2_g$	$e^3t^3_2$	1000	440	47.6	31.4	16.3
	Co^{+3}	^5D	t^6_{2g}	$e^3t^3_2$	—	780	188	107	81*
7	Co^{+2}	^4F	$t^5_{2g}e^2_g$	$e^4t^3_2$	1000	440	71.5	62.7	8.8
8	Ni^{+2}	^3F	$t^6_{2g}e^2_g$	$e^4t^4_2$	860	380	122.4	27.2	95.2
9	Cu^{+2}	^2D	$t^6_{2g}e^3_g$	$e^4t^5_2$	1300	580	92.8	27.6	65.2
10	Zn^{+2}	^1S	$t^6_{2g}e^4_g$	$e^4t^6_2$	0	0	0	0	0

The data given are:
1. Number of d electrons
2. Transition metal ions
3. Free ion Russell-Saunders ground (spin-orbit coupling is neglected in the term designation)
4. Electron configuration of octahedral ground state
5. Electron configuration of tetrahedral ground state
6. Dq values for octahedral hydrates of the ions
7. Dq calculated for tetrahedral coordination
8, 9. The thermodynamic stabilization in octahedral or tetrahedral fields
10. The octahedral site preference, or the difference between columns 8 and 9
* The octahedral site stabilization of Co^{+3} was estimated from the heat of hydration increment caused by the crystal field, and the tetrahedral site stabilization was taken to be the same as for Cr^{+3}.
SOURCE: T. M. Dunn, D. S. McClure, and R. G. Pearson, "Some Aspects of Crystal Field Theory," Harper & Row, New York, 19965, p. 82. Used with permission.

is stabilised to the extent of 1.33 Dq$_{oh}$ to cause an inverse structure to be formed.

Not all metal ions of the first transition metal series form a spinel which has an inverse structure. All the chromium spinels ACr_2O_4 have the normal structure as a result of the strong octahedral site preference of Cr³⁺. Further examples of spinels are listed in Table III. When applying the crystal field theory, one must remember that the structure of the oxide films, forming on the construction materials, is mainly governed by the operation environment. However, as soon as the transition metal ion is incorporated into the spinel structure, by using crystal field theory, it is possible to obtain an estimate how it will affect the crystal system. The oxide growth itself depends also on the ion transport through the oxide which is governed significantly by the defect concentra-

tion in the oxide film. This is discussed in some detail in the next chapter.

5.1.4.4 Defect structures in oxides

Solid materials are never perfect at temperatures above absolute zero but contain imperfections or defects in their structure. In spite of the often low concentration of defects, many important properties of solids are governed by their presence in the lattice. For example, the diffusion of or conduction by ions and electrons in crystalline compounds depend on the defect concentration in the lattice.[31]

In general, vacancies in an oxide lattice can result from imperfect packing during the original crystallisation or they may arise from thermal vibrations at elevated temperatures. Vacancies can be single or two or more of them may conden-

Table VI. *Relative crystal field stabilisation energies (CFSE) and resulting octahedral site stabilisation energies (OSSE) for various electron configurations.*[28]

Configuration	CFSE, tetrahedral complex		CFSE, octahedral complex, (Dq_{oh})	OSSE kJ/mol
	Dq_{td}	Dq_{oh}		
d^1	6	2.67	4	1.33
d^2	12	5.33	8	2.67
d^3	8	3.55	12	8.45
d^4	4	1.78	6	4.22
d^5	0	0	0	0
d^6	6	2.67	4	1.33
d^7	12	5.33	8	2.67
d^8	8	3.55	12	8.45
d^9	4	1.78	6	4.22
d^{10}	0	0	0	0

sate into a multi-vacancy. The presence of a vacancy does not mean that one lattice site is vacant while all the surrounding lattice particles remain in their original positions. However, it is possible that the neighbouring particles are moved from their original positions so that a certain distortion of lattice occur near the vacancy but at a greater distance the lattice is unperturbed.[29,32]

Behaviour of the lattice atoms on the surface of the crystalline compound differs also from that in the bulk. The surface atoms have neighbouring atoms only on one side. Therefore, they have a higher energy and they are less firmly bonded than the internal atoms. If additional atoms were to be deposited on the surface atoms, energy would be released just as it is released when two individual atoms are combined.[33] Stacking faults, internal surfaces (i.e. grain boundaries), twin boundaries and different types of dislocations belong to line or plane defects. They may also offer preferential pathways for the transport of species in the film.[30,33] A comprehensive consideration of line and plane defects is beyond the scope of this survey.

5.1.4.5 Mechanisms by which zinc affects activity incorporation

A general observation in all the reported zinc tests has been that Zn injection to high temperature water results in thin oxide layers with low visible porosity on new metal surfaces. In addition, the already existing oxide films do not grow in thickness, partly because corrosion product deposition

from the solution is minimal.[67,82,83,84,85] It has been postulated that zinc somehow decreases the defect concentration in the spinel structure by occupying existing holes in spinel lattice. This should slow down the ion transport though the oxide, leading to a reduced rate of oxide growth and the formation of thinner oxide films. [46,59, 66,67] The lack of thick deposited oxide film is likely to contribute to the observed low in activity levels in the existing oxides during Zn injection periods. However, the exact mechanisms by which zinc reduces activity incorporation into the oxide films are not yet known. It has been postulated that Zn may either replace the active and inactive cobalt from the oxide[46] or may block the adsorption sites for ^{60}Co pickup.[52,59,65]

As mentioned in the previous chapter cations can be placed in the spinel structure either in tetrahedral or octahedral positions. Co as well as Zn can be considered as dopant ions in the oxide structure. To calculate displacement energies required to replace one ion with another, the following energies are required: (i) Madelung and short-range energies, (ii) the crystal field stabilisation energy for an ion in a crystal site. These calculations show that zinc has a very strong stabilisation in tetrahedral sites, and in fact it should be able to displace all other divalent cations from the chromites. This could explain the function of zinc in promoting thinner and more protective oxide films and inhibiting the incorporation of cobalt into the chromium rich oxide film.[47] Some laboratory experiments have shown that displacement

reaction is possible, but a chromium rich oxide film (throughout the film) is required for suitable solid state reactions to occur. In addition, high zinc concentrations as ZnO should exist on the oxide surface.[85] If the chromium rich oxide film has incorporated cobalt ($CoCr_2O_4$) and zinc ($ZnCr_2O_4$), an addition of ZnO to a stoichiometric mixture of $CoCr_2O_4$ and $ZnCr_2O_4$ may result in the formation of CoO and Co. Due to the high solubility of these oxide phases, the cobalt concentration in the aqueous phase should increase by almost four orders of magnitude. This would automatically lead to a lower cobalt concentration in the oxide film.[81]

An other way for zinc to affect is to compete with cobalt for occupancy of surface sites as the oxide is formed and thereby effectively block the routes for cobalt incorporation.[18] This can be an important intermediate stage in the incorporation of cobalt and zinc into the oxide film.

It has been suggested that the transition metal ions at concentrations higher than 10 ppb would practically saturate the available adsorption sites for [60]Co. Although ^{60}Co could compete with all ions, the total amount of ^{60}Co which could reach the reaction/adsorption/ion-exchange sites would be significantly diluted by the competing ions. Also the fact that zinc ions have shown to significantly retard the film growth leads automatically to a smaller number of available adsorption sites for ^{60}Co which are limited by both the thinner film and the competition from zinc ions.[52,59,65] The blocking of the adsorption site may control, if the solid state reactions explained above can not occur or are very slow. The different mechanisms could explain why some research groups have made totally different observations.[85]

5.1.5 Zn water chemistry and stress corrosion cracking

As discussed in the chapter 4.2, the models developed for SCC assume that the anodic and corresponding cathodic reactions contributing to crack growth occur partly on or in the oxide films. Thus, the rates of these reactions may control the crack propagation rate, in which case the properties of the oxide films play a crucial role in determining the susceptibility of the material to SCC. The crack initiation always involves rupture of the oxi-

de film on the construction material. Therefore, a deliberate injection of some additional ions, such as Zn, into the coolant affecting the behaviour of oxide films is likely to have an impact of the susceptibility of the materials to SCC.

5.1.5.1 Effect of Zn on PWSCC of Inconel 600 in PWRs

Primary water stress corrosion cracking (PWSCC) of Inconel 600 components has become an increasing problem in western PWRs. Even though these cracks have not been a safety issue, they pose a significant reliability and economic concern. The first PWSCC indications were observed in U-bend steam generator tubes. The SG tubing is a physical boundary between the primary and the secondary waters. Hence it is essential that the integrity of the tube remains secured. During the last years cracking has also occurred in various types of penetrations, such as instrument and pressure vessel penetrations, pressuriser heaters and nozzles. The cracking in PWSCC is controlled by a combination of stresses, environment (temperature, pH_T, $[H_2]_{gaseous}$ etc.) and material microstructure (distribution of carbides, grain size, etc.). [19, 101] The initiation needs an induction time, i.e. the time needed for an apparently smooth surface to develop a crack. This is followed by crack propagation, which finally leads to tube rupture.

Early studies by Esposito et al. showed that zinc injections (50 ppb doses as zinc borate) appeared to significantly affect the stress corrosion cracking behaviour of Inconel 600 MA steam generator tubing material.[20] These tests were carried in typical PWR environments with 25 cc/kg of hydrogen using highly stressed U-bend specimens (RUBs). In the tests where Zn was injected into the water formed oxide layer on all specimens the was thinner. The surface film analysis showed that Zn existed throughout the film. In addition, there were significant changes in the PWSCC initiation times in all materials between the samples which were exposed to waters with and without Zn as shown in Figure 13.

The time for PWSCC initiation of the specimens made from the heats 1019 MA and 96834 MA in zinc containing water was 2.5 times longer than for the specimens exposed to the coolant without zinc. The thermally treated specimen made of heat 752537 TT did not experience

PWSCC initiation at all in zinc containing water, even though 50% of the specimens exposed to high temperature water without Zn experienced the SCC initiation. Zinc seemed also to reduce the relative extent of the cracking, in terms of less crack density and shorter crack lengths.[20]

A more detailed analysis of the same specimens done by Byers et al. revealed that iron and chromium concentrations in the oxide of Inconel 600 were higher when also Zn was incorporated into the oxide film. The analysis of chromium binding energies indicated that a chromium–zinc phase was possibly formed.[68]

Due to the potential benefits of zinc additions on mitigating PWSCC of Alloy 600, the following demonstration was carried out at Farley 2 unit. The zinc concentration (added as zinc acetate) was kept at 40 ppb in the primary coolant for 9 months during the cycle 10. Eddy current measurements were made from all hot leg tube ends at the top of the tube sheet during the outage. These measurements showed that the rate of PWSCC had decreased during the presence of Zn. The detailed analysis of the formed oxide layers asserted that zinc was incorporated into the oxide in the same extent as in the laboratory tests during which decrease of PWSCC had been observed. However, due to the rather short zinc injection period and possible contributions from other actions taken,
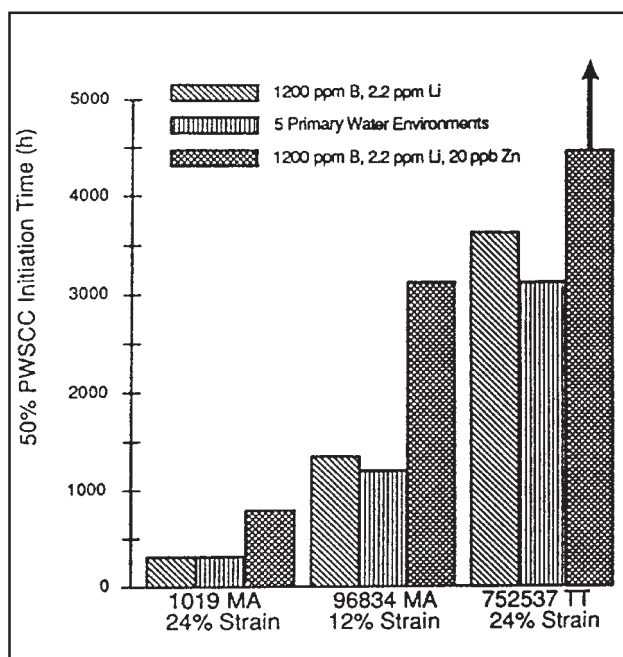
no firm conclusion on the benefit of zinc addition could be drawn. These referred actions taken included shotpeening of the hot leg tube ends in 1987 which most likely had resulted in a declining number of new indications of PWSCC since 1990. [76,77]

Bergmann et al. have reported results from the crack growth rate tests using passively loaded CT specimen made of Inconel 600.[77] No crack propagation was observed in the specimens exposed to the coolant containing zinc, whereas all specimens in the coolant without zinc exhibited crack propagation. However, quite different results were observed by Airey et al.[105] They dosed 40 ppb of zinc (as zinc acetate) into typical PWR primary coolant but did not see any effect of zinc on the SCC initiation times with the used specimens (reverse u-bend and bent beam specimens). The crack growth rate measurements (using compact wedge open loading specimens) did not indicate any benefit from the zinc injections either. However, the test results showed that the formed oxides were thinner and enriched with chromium due to the zinc addition.

5.1.5.2 Effect of Zn on IGSCC in BWRs

Andresen et al. [107,108] have studied the effects of Zn on stress corrosion cracking of different alloys under the BWR conditions using CT fracture mechanics specimens. The specimens were exposed to high purity water containing different amounts of oxygen and impurities under study at 288 °C. Zn concentrations of 5 to 100 ppb (as ZnO) were found to reduce crack growth rates in all studied materials. However, the factor of improvement with Zn addition was usually lower than that obtained when changing from NWC to HWC. Some of the results are summarised in Figure 14, which shows the crack growth rate (CGR) as a function of corrosion potential and zinc concentration.

The results clearly indicate that zinc had the most significant effect on the CGR when the corrosion potentials of the studied materials were around 0 mV$_{SHE}$. This was the low limit of the investigated potential range during the Zn tests. At higher potentials the difference between crack growth rates in non-Zn and in Zn containing coolants was less obvious, Andresen et al. related

Figure 13. *Mean PWSCC initiation times for different conditions of Inconel 600 reverse U-bend specimens.[20]*

this observation to two issues: first, at higher corrosion potentials, the potential gradient within the crack becomes larger which increases the anion concentration within the crack but drives more cations (including Zn^{2+}) out of the crack. Second, at higher potentials the crack growth rates in general are higher therefore providing less time for Zn to have effect on IGSCC. The largest effect of Zn resulted from long term exposure, low corrosion potentials and long hold times between unloading cycles.

Similar test results were also obtained by Hettiarachchi et al.[109] They reported that if the oxygen concentration was reduced below 100 ppb, the probability of IGSCC to occur could be significantly reduced in the presence of zinc (dosed as ZnO). This improvement existed even at very low zinc concentrations (3 ppb), and no additional benefit was observed using higher Zn concentrations (100 ppb). They measured also the corrosion potential of the specimens as a function of oxygen concentration with and without Zn. In the presence of zinc, the corrosion potential of specimens decreased approximately 70 mV in solutions containing high O_2 concentrations. With low oxygen concentrations, the decrease in corrosion potential was even larger (roughly 120 mV), as shown in Figure 15.

It was concluded that addition of Zn provides the benefit by moving the corrosion potential into more negative values similar to hydrogen.[109] However, the effect of zinc was significantly small-er. This was clearly shown in the test in which the water contained 200 ppb of oxygen, 100 ppb Zn and 10 ppb hydrogen. The crack growth rate of Alloy 182 weld metal was reduced only when excess of hydrogen was present in the water.[110] This agrees with the results reported by Andresen et al. (see above).

According to the slip-dissolution model, an increase in oxide film rupture strain or re-passivation kinetics of a new surface at the crack tip will improve the resistance to IGSCC or reduce the crack growth rate. The results of Angeliu et al. show that as the zinc concentration in the coolant increases, the oxide film rupture strength of AISI 304L SS increases as shown in Figure 16.[111]
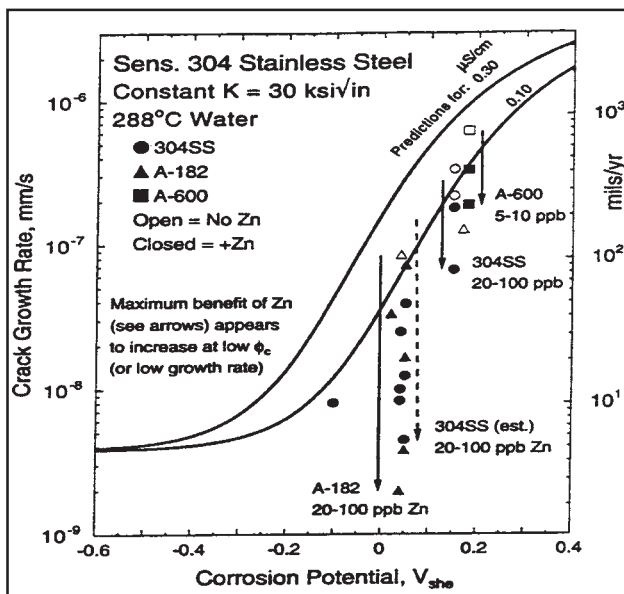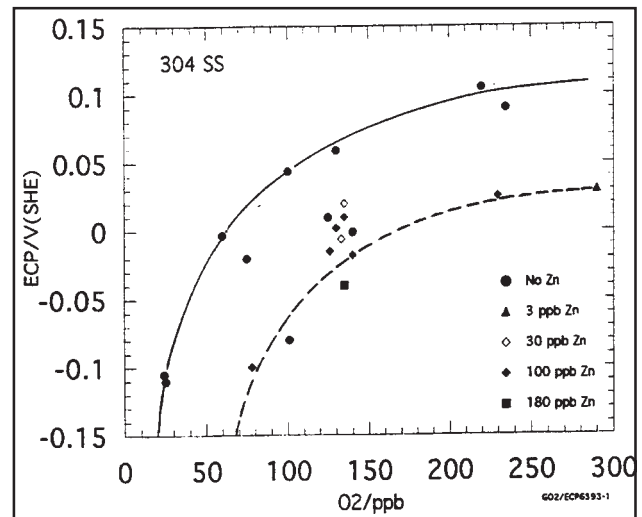

Figure 15. *The influence of zinc on the corrosion potential of the specimen at different dissolved oxygen levels.[109]*

Figure 14. *Overview of the crack growth rate response vs. corrosion potential and Zn addition.[108]*
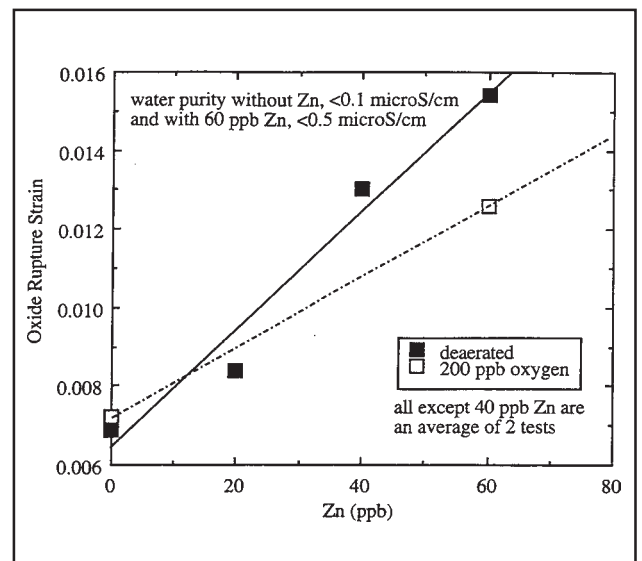

Figure 16. *Oxide rupture strain as a function of Zn for type AISI 304L SS exposed to 200 ppb O_2 and deareated high purity water up to 166 h at 288 °C. [111]*

In addition, long term tests showed that an exposure over 300 hours to a solution containing only 20 ppb of Zn resulted in similar oxide rupture strain as with 60 ppb of zinc in short term tests. High zinc concentrations provide a greater driving force and availability for Zn incorporation. However, similar effects can be obtained with low Zn concentrations if long enough exposure times are allowed.

Angeliu et al. have also measured the re-passivation kinetics of Fe-12 Cr steel in high temperature water. In all the studied environments, the measured re-passivation current densities were similar immediately after the film rupture with and without Zn.[111] This has been verified also with more recent measurements, which showed that re-passivation kinetics of Inconel 600 (up to ~100 s) were not affected by Zn addition.[112,113] However, after 10^4 s the measured current densities of Fe-12 Cr steel were lower in the presence of Zn. This indicates that the study of the mechanisms by which zinc is changing or affecting electrical and mechanical properties of the oxide films, requires long enough exposure time.

5.1.5.3 Comments of zinc effects on SCC

As discussed in the chapter 4.2, the properties of the oxide films on construction material surfaces may have a strong influence on SCC. The thicknesses of the oxide films have been lower in all zinc injection tests than in the tests without zinc.[67] It has been postulated that Zn^{2+} slows down the iron transport though the oxide, leading to a reduced rate of oxide growth and to the formation of thinner oxide films. It is assumed that this kind of thinner oxide is less likely to break and expose the base metal to the environment than a thicker oxide with a higher defect concentration.[106] Therefore, the influence of zinc on SCC is likely to be due to its incorporation into the oxide films. To be able to affect cracking process zinc has to reach the oxide surface in the crack and have enough time to be incorporated into the oxide. The probability for these processes to take place depends also on the corrosion potential as described below.

At higher corrosion potentials, the potential gradient within the crack becomes larger and increases the anion concentration within the crack and drives more cations (including Zn^{2+}) out of the crack. Therefore, the laboratory results which show that at higher corrosion potentials the difference between crack growth rates in non-Zn and with Zn containing coolants was less substantial, are consistent with the ion distribution within the crack.[107,108] It has been shown both in laboratory and in operating power plants that addition of Zn (as ZnO) increases pH_T of the high purity water moving the ECP of the materials slightly in the negative direction. This decreases the potential difference in the water between the crack mouth and crack tip and enables more zinc ions to be transported into the crack surfaces.[109]

Secondly, at higher corrosion potentials the crack growth rates in general are higher providing therefore less time for Zn to have an effect. The largest effect of Zn resulted from long term exposure, lower corrosion potentials and long hold times between unloading cycles.[107,108] The re-passivation kinetics of fresh crack surface in high temperature water were similar with and without Zn immediately after film rupture. This indicates that the mechanisms by which zinc is changing or affecting the electrical and the mechanical properties of the oxide films, requires long enough exposure time in zinc containing coolant. On the other hand, higher zinc concentrations provide a greater driving force and availability for Zn incorporation resulting accordingly, shorter exposure times to observe the benefits.[111]

5.1.6 Detrimental effects of zinc

As discussed in the chapter 5.1.1.1, the plants dosing natural zinc have observed that the activation of ^{64}Zn to form ^{65}Zn adds to the inventory of activated corrosion products in the plant. Zn injections have also resulted in the deposition of hard, tenacious crud on fuel cladding surfaces. For some reason eddy current measurements have given extraordinary high values for oxide thickness on fuel cladding surfaces. In addition, the restructured crud deposits on fuel cladding surfaces have been reported to be resistant to brushing with stainless steel bristles. The changes in crud loading during the zinc injection periods at Hatch-1 unit are shown in Figure 17. The zinc concentration in the oxides on cladding material has increased from 5% up to 20%. Prior to zinc injections, the Zn source had been the brass condenser tubes. The deposits were analysed to have a structure typical for

magnetite, but based on the chemical analysis the composition of the spinel was most likely $ZnFe_2O_4$. Crystallographic analysis also showed that the formation of spinels in the fuel deposits increased with increasing zinc concentrations in the reactor water.[91]

The rod average crud loading on the Hatch 1 rods was relatively low, as shown in Figure 17, partly due to low feed water Fe concentrations. On the other hand, the crud loading on the Hope Creek rods was relatively high, because of a higher feed water iron input (6–8 ppb). In general, the thermal conductivity of iron based oxides in solid form is higher than that of the zirconium oxide on fuel cladding surface. However, if dry steam forms within a delaminated oxide or tenacious deposits, the thermal conductivity could decrease by a factor of 8, increasing the temperature of the fuel cladding. Thus, the combined effect of increased tenacity and crud loading with increasing burn-up could become significant.[61,91,92]

In PWRs, the fuel performance has been less sensitive to water chemistry conditions, mainly because of the negligible surface boiling. Addition of Zn to the primary coolant has been suggested to present a potential risk for fuel reliability. However, no detectable effects on cladding corrosion have been observed at Farley-2 unit after Zn additions for 9 months. In addition to this plant demonstration, an in-core loop test was carried out at Halden test reactor to provide an early warning of any deleterious effects of zinc injections on the fuel cladding behaviour. Both fresh and re-irradiated fuel segments were exposed to

Table VII. *Chemical decontamination results in zinc addition plants.*

Plant	BRAC Pt DF	Pre/Post Dose rate (mR/hr)
Millstone Pt 1	22	217/10
FitzPatrick	11	113/10
Monticello EOC-14	25	613/25
Monticello EOC-15 BRAC Pts	7	3 pts - 400/60 4th pt - 3000/450
All Points	~3	1250/430
Hatch 1	8	180/22

PWR conditions with 50 ppb of Zn. The results showed no apparent effects of zinc on either corrosion or hydriding of the low tin and standard Zircaloy cladding. Although no effect of Zn is anticipated based on the experience from Halden tests and Farley-2 results, continuous monitoring of fuel is recommended if the zinc injections are carried out.[76,77,93,94]

One of the early concerns in the plants using zinc dosing was whether the oxide films formed during the presence of zinc could be decontaminated using currently available chemical processes. In the past years, decontaminations have been carried out in several plants and they have been highly successful in all but one case, as shown in Table VII. However, the precise cause for the ineffective decontamination is not yet known.[61]
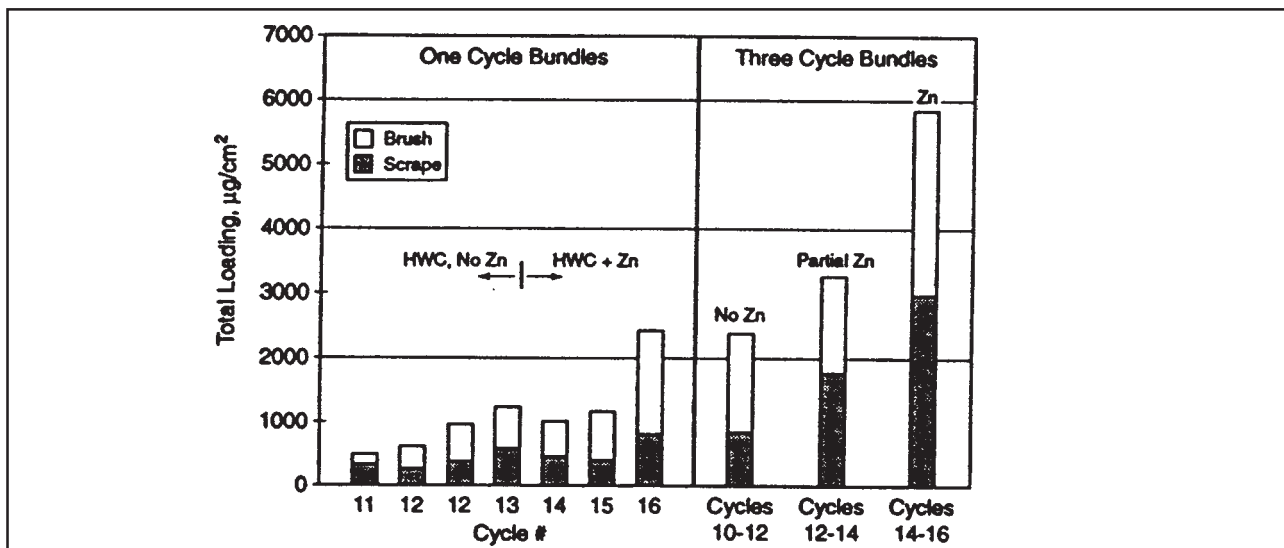

Figure 17. *Crud loading in Hatch-1 fuel bundles under HWC chemistry with Zn and no-Zn addition.[91]*

5.1.7 Alternatives for zinc injection

To overcome the problems associated with the use of zinc water chemistry, several research groups have studied alternatives for zinc by evaluating the general properties and characteristics of different metal ions. A possible way to prevent deposition of cobalt into the oxide surfaces is to maintain its concentration in the aqueous phase as low as possible compared with the concentrations of other ions which compete with Co for adsorption or lattice sites. According to Niedrach and Stadder the order of incorporation of transition metal ions into the existing oxides is Ni $\cong$ Co > Zn > Mn.[52] This was supported by the results of Lin et al., who showed that both zinc and nickel can effectively suppress the ^{60}Co build-up in the oxide film as shown in Figures 18 and 19. It has been suggested that other transition metal ions such as Mg^{2+}, Mn^{2+} may behave similarly.[52]

The results of Osato et al. indicated that the effects of Ni^{2+} dosing into the high temperature water decreases the up-take of cobalt into the oxides under HWC environments. The activity build-up on electropolished and as-received stainless steel samples became lower during Zn and/or Ni addition when compared to the samples, which were exposed to the high purity coolant. However, the activity in-corporation into the carbon steel

samples was not inhibited to the same extent.[87]

Korb et al. have also studied alternatives for zinc. The remaining elements of interest left after their evaluation were Ca, Mg, Mn and Sr. Furthermore, the results showed that for trivalent cations the chromites have higher stability than the ferrites. With regard to bivalent cations, Zn, Co, Ni, Fe, Mg and Mn, the trends are not so systematic. In addition, the reaction conditions had a considerable influence on the order of stability of the spinels involved. However, some conclusions were drawn: Co spinels appered to be more stable than the spinels containing Fe and Ni. Moreover the affinity of Zn for spinels was suggested to be even higher than that of cobalt.[81]

Uetake et al. studied also how different ions affect the deposition of activity into the oxide films on AISI 316 SS. They found out that Al has almost same reducing effect as Zn as shown in Figure 20. Mg^{2+} was also studied with same molar concentration, but no inhibition of activity incorporation was seen.[90]

Iron injection in BWRs has been widely used in Japan as well as in some plants in USA and Europe. The idea is to control the composition of crud on fuel by means of controlling the concentrations of Ni and Fe in the coolant, in order to minimise the concentrations of soluble ^{60}Co and ^{58}Co. The crud on the fuel consists mainly of Fe
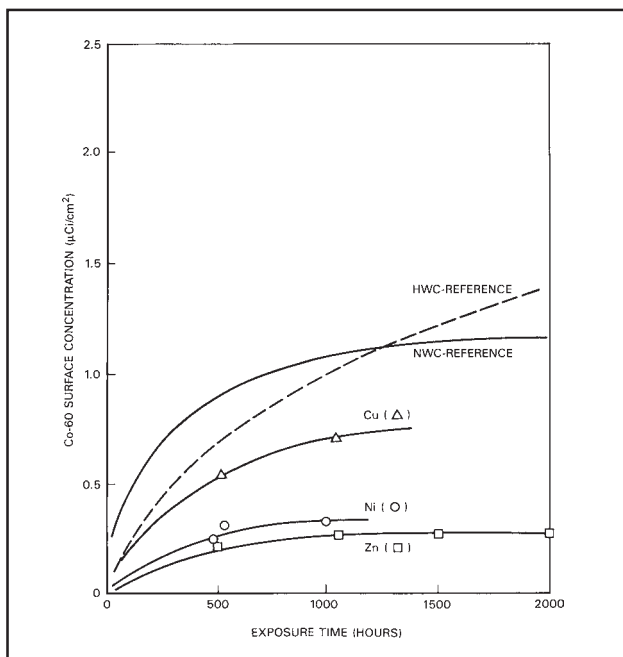

Figure 18. Comparison of ^{60}Co deposition on as-received AISI 304 SS samples under NWC conditions with metallic ions at 15 ppb.[52]
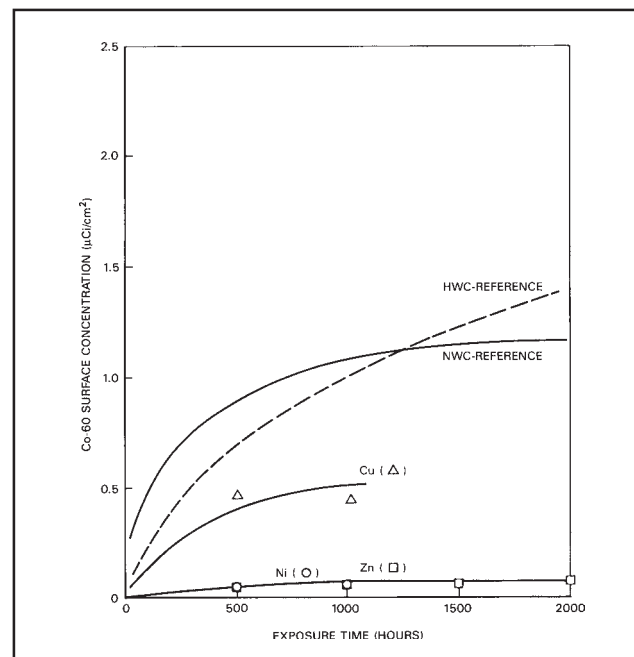

Figure 19. Comparison of ^{60}Co deposition on as-received AISI 304 SS samples under HWC conditions with metallic ions at 15 ppb.[52]

and Ni, which have been deposited as $NiFe_2O_4$. If the iron to nickel ratio in the coolant is two to one, Fe and Ni will form nickel ferrite, from which cobalt can replace nickel to some extent. This leads to lower levels of activated cobalt in the coolant due to the low solubility of the spinels. Too small amount of Fe in the coolant results in the formation of NiO and subsequently to a higher release of ^{60}Co and ^{58}Co. The effects of iron injection on the concentrations of activated cobalt isotopes and nickel in the reactor water are shown in Figure 21.[88]

However, some Swedish results have shown that iron injection has led to increased activity build-up in the oxides on SS piping surfaces.[88] This has been reported to be due to the changed oxide structure in the primary circuit. During the low iron concentration in the coolant, typical BWR oxide loses the outermost hematite layer and leaves behind a nickel ferrite oxide layer, which reduces the tendency of the surface to take up Sb-124.
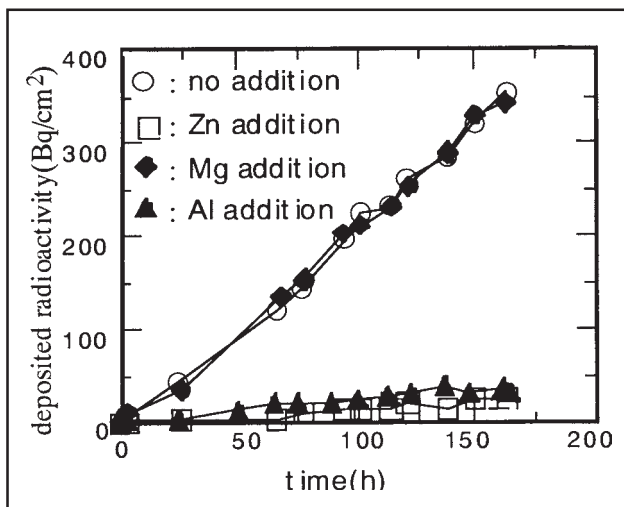
In some Japanese plants ^{60}Co concentrations in the coolant have increased even though the Fe/Ni ratio has been optimised. The reasons are still unknown but several possible mechanisms have been proposed, such as the adverse effect of not pre-oxidised fuel surfaces and higher than normal Cr concentrations in the coolant.[89]. Uetake et al. confirmed that the fuel surfaces must have an existing Fe crud before the iron injections remain effective. The metal ions deposit as hematite and nickel and Co monoxides on fuel cladding surfaces as a result of growing steam bubbles. As the bubble reaches a critical size it will leave the surface. A part of the deposits re-dissolve and the rest of them form ferrites. This process allows incorporation of Co into the oxides. If enough Fe exists in the solution more Co will be incorporated into the stable spinel.[90]

Nevertheless, the overall understanding of the processes within the oxides is still lacking. This complicates the optimisation of primary coolant conditions to further decrease dose rates at operating power plants.

5.2 Noble metal water chemistry

5.2.1 Principles of noble metal water chemistry

As discussed in the preceding chapters 4 and 4.2, the susceptibility for the stress corrosion cracking of construction materials in BWRs can be mitigated by adding hydrogen into the feed water. This decreases the levels of oxidising species and thus lowers the corrosion potential (ECP) of the construction materials. This has been shown to apply both under irradiated (IASCC) and unirradiated (IGSCC) conditions as shown in Figures 22a and 22b.[114]

Figure 20. The effect of metal ion additions on Co incorporation into existing oxides.[90]
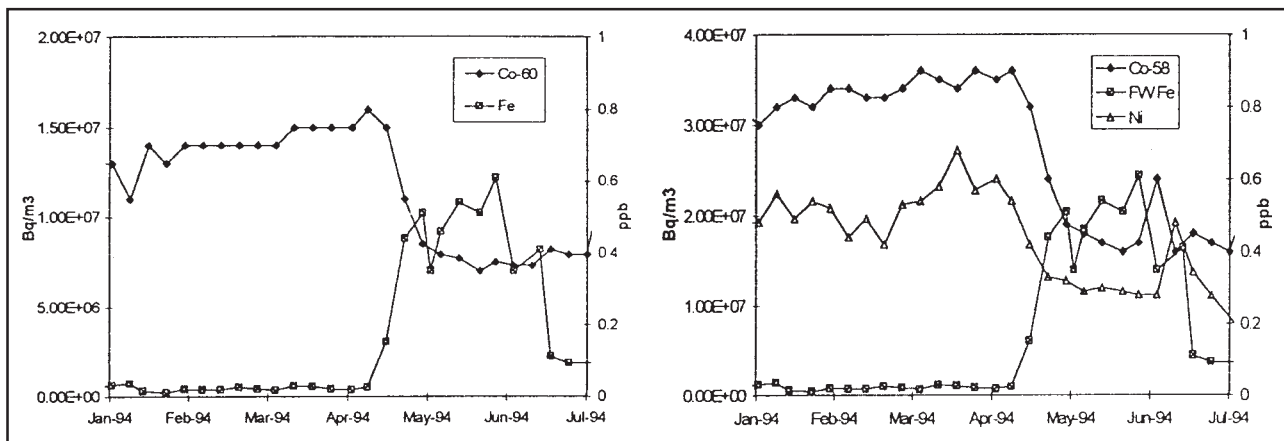

Figure 21. Effect of iron injection on cobalt isotopes in reactor water at Forsmark 3.[88]

The low corrosion potentials of construction materials are obtained only if all oxygen which diffuses onto the material surface is consumed by the formation of water. The minimum amount of hydrogen needed (C_H:C_O = 2:1) corresponds to a 1:8 C_H/C_O weight ratio. Therefore, the hydrogen threshold concentration is ≥ 1/8th of the oxygen concentration expressed for example in ppb. Laboratory experiments have shown that even lower hydrogen concentrations (C_H:C_O = 1:12) are sufficient to decrease the measured corrosion potentials, because the diffusivity of hydrogen in the water layer next to the oxide surface is higher than that of oxygen or hydrogen peroxide. The mechanism by which catalysed surfaces behave is shown in Figure 23.[116]

The measured or calculated ECP depends on:

(1) the exchange current densities (i_o) for different reactions (i_o, reversible reaction rate at equilibrium), (2) the rate constants for reactions which determine the activation controlled polarisation response and (3) the diffusion coefficients for gases and ions, which determine the diffusion controlled response (or the limiting current densities, i_L shown in Figure 23). These parameters are dependent on the studied system. They are affected by O_2, H_2, H_2O_2 concentrations, the surface condition, the surface composition (stainless steel, noble metal modified alloys, etc.) and the flow rate of bulk solution.[117]

The corrosion potential is governed by a balance between the total oxidation and reduction reaction rates that occur on the material surface. In a simplified situation as shown in Figure 23,
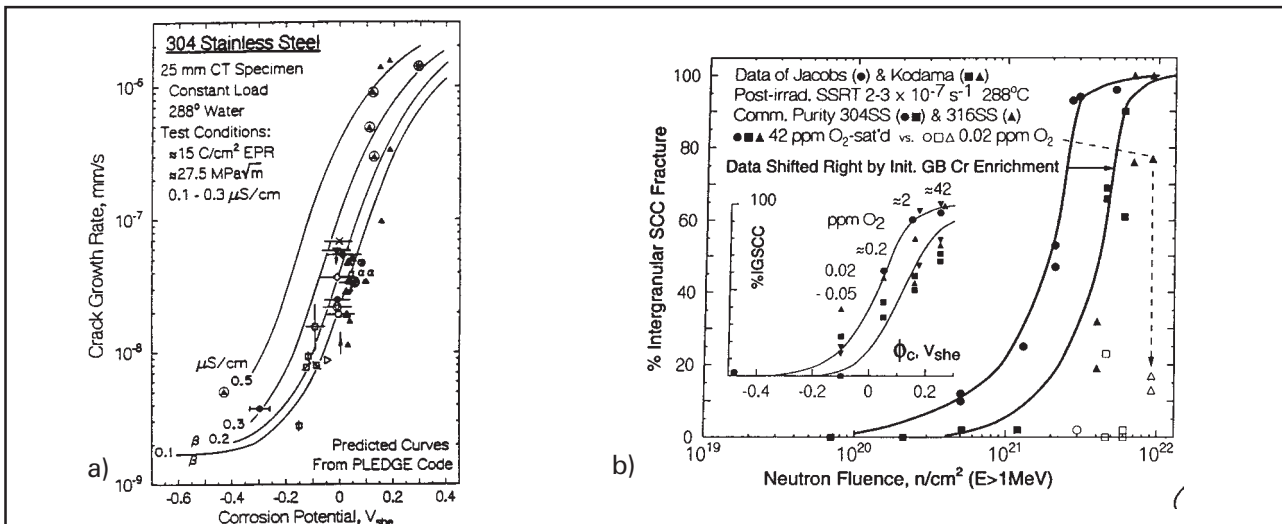

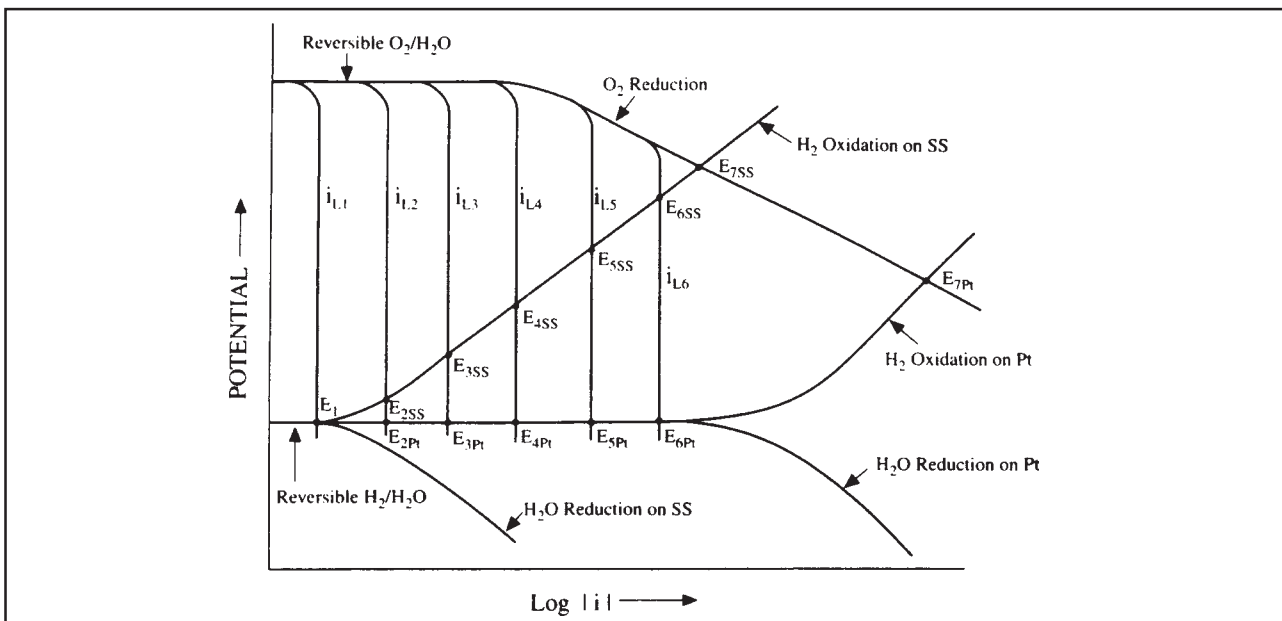**Figure 22.** *Observed and predicted crack growth rate as a function of corrosion potential.[114]*

Figure 23. *Schematic Evans diagram showing the intersection points for the curves of oxygen reduction and hydrogen oxidation on stainless steel and Pt.[116]*

the corrosion potential ($E_{i,SS/Pt}$) is fixed to the potential, where the O_2 reduction curve intersects the H_2 oxidation curve. Typically, the construction materials have a low exchange current density for O_2 reduction and H_2 oxidation. This means that even with moderate oxygen concentrations the corrosion potentials of different materials can rise to fairly positive values as shown in Figure 23 by the points $E_{3SS},...,E_{7SS}$. Low potentials can be achieved only with very low oxygen concentrations where O_2 reduction becomes diffusion limited (like the curve for i_{L1} in Figure 23) and intersects the H_2 oxidation curve at a current density, lower than the exchange current density for H_2 oxidation. However, catalytic surfaces have a high exchange current density for H_2–H_2O oxidation and reduction. Therefore, the corrosion potential of Pt stays low even at fairly high oxygen concentrations as shown in Figure 23 by the points $E_{2,Pt},...,E_{6,Pt}$. This is the basic phenomenon which explains the efficiency of noble metal coatings in obtaining low corrosion potentials of the in-core components even with low hydrogen dosing into the feed water.

Noble metals have been used as catalytic surfaces in science for a long time. If the construction material surface could be made to behave like a noble metal surface, it would catalyse the recombination reaction between hydrogen and oxygen, decreasing the corrosion potentials with reasonably low hydrogen concentrations. This would also
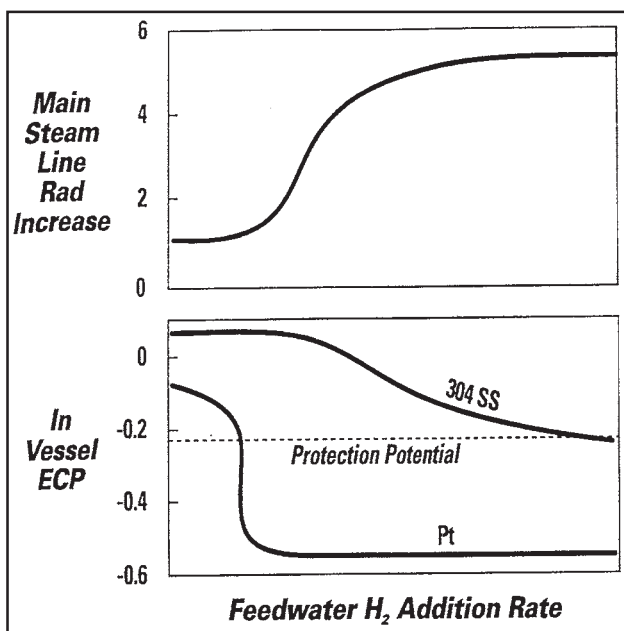
result in lower main steam line dose rates as shown in Figure 24. In plant applications the amount of hydrogen needed to reduce potentials enough has shown to be plant specific and is always in excess of the stoichiometric amount required for the recombination with oxygen to form water. In the out-of-core regions, hydrogen additions have resulted in low enough corrosion potentials, but the materials in in-core locations can be protected only with much higher hydrogen concentrations.

An additional benefit of a lower corrosion potential is higher acceptable impurity levels in the coolant without effect on the crack growth rates as shown in Figure 25. During this test the conductivity was changed from 0.11 μScm^{-1} to 0.86 μScm^{-1} without any effect on crack growth rate. This shows that low corrosion potentials provide high tolerance to severe water chemistry transients (e.g. impurity in-leakage).

5.2.2 Different types of noble metal coatings

A variety of different types of noble metal coating techniques have been developed for improving the catalytic properties of oxide surfaces on structural materials. The noble coating on the metal surface can be obtained using electro- or electroless plating and vapor deposition. However, these techniques can be applied only in autoclaves or in other laboratory environments. Surface analysis has indicated that typically several weight percent of
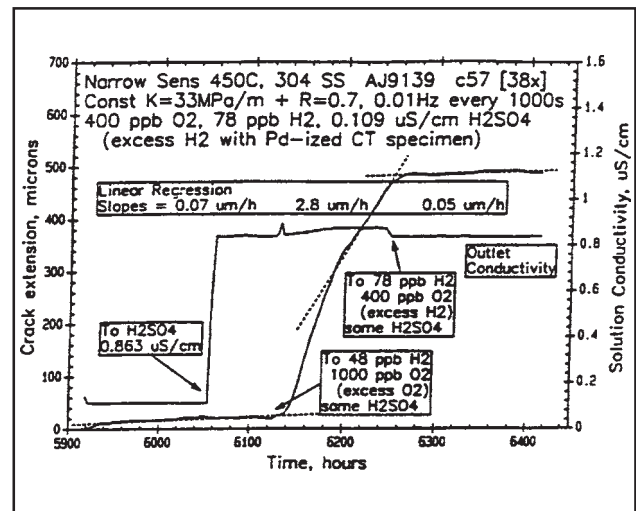
Figure 24. Schematic basis for the use of noble metal technology in BWRs.[115]

Figure 25. Response of Pd coated CT specimen at low corrosion potentials and high conductivity values.[117]

the amount of noble metal was incorporated into the oxide film to the depths of several tens of nm. However, it is also likely that some areas had thinner coverage of noble metal.[117,118]

More dilute noble metal layers can be produced by using thermal spray coating of noble metal alloy powders or by direct alloying of the material itself. Under water thermal spray coating techniques can be carried out in high purity water either in shallow or deep waters. The catalytic properties of metal surfaces have been obtained by using hyper-velocity oxy-fuel (HVOF) and plasma spray (PS) coating techniques. The used coatings consisted of AISI 309L SS powder with 0.42% of Pd and Alloy 82 with 0.4% of Pd. In the HVOF process, gas mixtures of propylene/oxygen or hydrogen/oxygen were used. In the PS process, a dc plasma arc is created in an inert gas (helium and/or argon) between anode and cathode, both in the torch head. The powder is fed into the ionised gas stream and is heated and accelerated towards the metal surface.[119] The results of Kim et al. show that HVOF and PS coatings responded fully catalytically in the presence of a stoichiometric excess of hydrogen in different oxygen concentrations. It has been reported that the corrosion potential of stainless steel increases more significantly by the addition of H_2O_2 when compared to the effect of oxygen. However, Kim et al. have shown that PS and HVOF coatings exhibited good catalytic behaviour in water containing 500 ppb of hydrogen peroxide when excess of hydrogen was added to the water.[120] These techniques have some limitations when applied in operating BWRs, because

of the poor accessibility of a large number of in-core components. For some components like the top guide, parts of the core shroud etc. these techniques seem to be very attractive.

Direct alloying of the construction materials can be used only in replacement parts. Nevertheless, the technique has been found to improve the catalytic efficiency for hydrogen/oxygen recombination in high temperature water with relatively small amounts of hydrogen.[121] Andresen et al. studied the crack growth rates of the noble metal alloyed stainless steels in high temperature water in different conductivity ranges and in different O_2 and H_2 concentrations. One set of results is shown in Figure 26.[122] The specimen was not sensitised and therefore higher conductivities were needed to increase crack growth rates, but the benefit of noble metal coating can be clearly seen from Figure 26.

A system wide approach could be the application of the noble metal chemical addition (NMCA) technique, in which the reactor coolant is used as the medium of transport for depositing small amounts of noble metal onto the oxide surfaces. The first verification tests with NMCA were carried out in autoclaves. The noble metal compound which was added into the water was either palladium acethylacetonate or palladium nitrate. During this high temperature water exposure the noble metal concentration in the water varied between 10 and 100 ppb. The effect of Pd NMCA on the corrosion potential of AISI 304 SS specimen in different hydrogen/oxygen molar ratios is shown in Figure 27.[110]
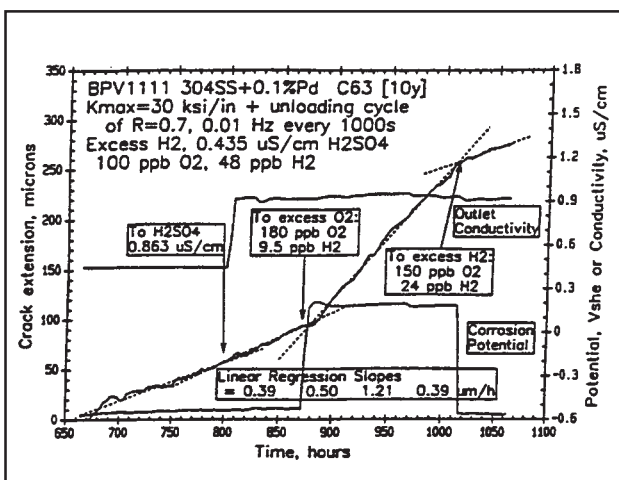

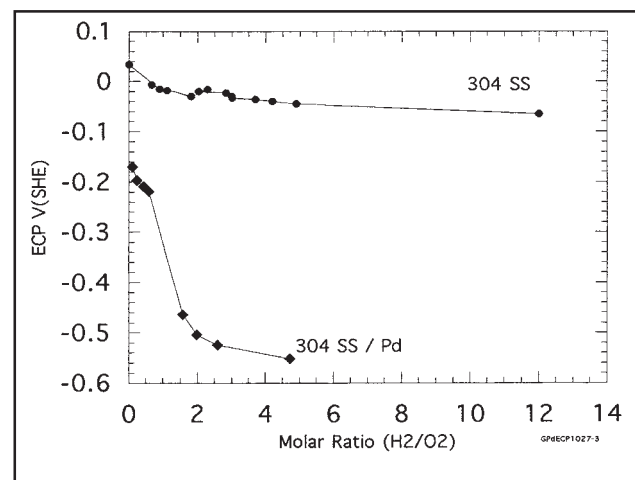*Figure 26. Crack length, corrosion potential and outlet conductivity vs. time for CT specimen.[122]*

Figure 27. Corrosion potential response of a Pd doped and a reference AISI 304 SS specimen to H_2/O_2 molar ratio.[110]

According to the AES results of Kim et al., Pd added as acethylacetonate was present in the oxide surface at a few atomic percents to the depths of about 400 Å.[124]

5.2.3 Long term stability

To be a viable process in operating BWRs, the applied coating should retain the catalytic activity over an extended period of time under high flow rates of the BWR coolant. In addition to this, the coating should withstand the changes from NWC to HWC. The results from the test, which was performed to verify the operation of the catalytic properties over the period to 12 months with water chemistry changes from normal to hydrogen water chemistry are shown in Figure 28.[123]

The ECP increases with increasing flow rate as shown earlier (Figure 1). The high flow rate itself could pose a risk in promoting erosion corrosion of the noble metal coatings. Kim et al. studied the effects of high flow rate and ultrasonic exposure to the catalytic properties of the exposed surfaces. They found out that one week exposure to high water velocities increased the ECP from –500 mV$_{SHE}$ to –250 mV$_{SHE}$.[124] A similar increase in potential was also observed after the ultrasonic tests.

To further improve the long-term stability of the noble metal coatings, a mixed noble metal application has been tested. Initial data shows that the durability of noble metal coatings can be improved by doping simultaneously several noble metals (e.g. Pt, Ir, Ru, Rh, etc.). The first laborato-
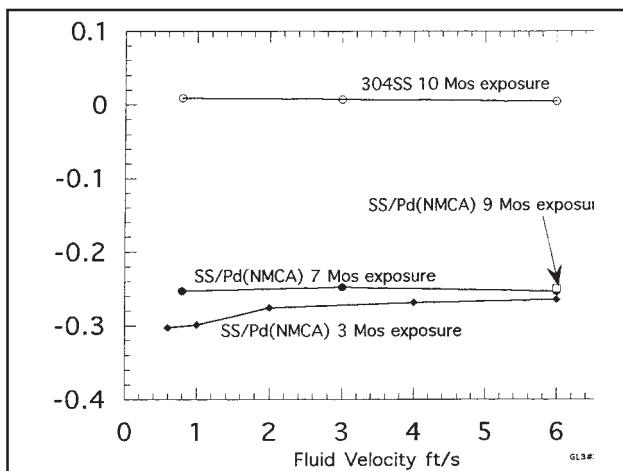

Figure 28. Corrosion potential response of Pd/SS after 9 months durability test under high flow.[123]

ry results have indicated even better catalytic activity of the mixed coated surfaces for the same flow velocities, indicating also better durability in high water flow rates.[124]

5.2.4 Effect of the operational environment

The plant observations have indicated that the change from NWC to HWC causes reduction in the oxide film thicknesses. This is mainly due to the enrichment of chromium in the film, which leads to lower corrosion rates of the base metal. However, results reported by Hettiarachchi show that film thinning during HWC operation does not affect the catalytic activity of the surface in prolonged exposure to HWC.[123]

Kim et al. studied the effects of Zn (as ZnO) and Cu (as CuSO$_4$) on the catalytic behaviour of noble metal coated surfaces.[125] They used 0.1% Pd alloyed AISI 304 SS steel samples. The results showed that both zinc (at 100 ppb range, not below) and copper increased the corrosion potentials of the specimens with some tens of millivolts. The conclusion was that Zn or Cu deposited on the surface film blocked either of the half-reactions occurring on the noble metal coated surface: O$_2$ reduction or H$_2$ oxidation. Because the ECP increased, they concluded that the rate of H$_2$ oxidation reaction was somehow decreased. The measurements confirmed that the recombination efficiency of O$_2$ and H$_2$ decreased by 10% when zinc or copper was injected into the high temperature water under excess of H$_2$. The analysis of the oxide showed that both Zn and Cu concentrations were highest on the outermost surface layers, but no significant difference was observed in the oxide particle density and size after Zn and Cu injections.

To find out how the NMCA would work on the surfaces in plants, in which crud deposition onto the core surfaces was high, a set of tests were carried out in laboratory environments. The results of Hettiarachchi et al. indicated that typical crud layers (sample which had been in operating plant for 10 years) did not affect the NMCA process and proper catalytic behaviour of the surface was obtained.[123] The test also verified that it is possible to use the NMCA technique to

successfully dope all in-core components. The electroless coating process has also been shown to work efficiently both on bare surfaces and on surfaces with old, representative oxide layers. No loss of catalytic activity was observed by Andresen et al.[117]

After the NMCA had been applied in the simulated crudding processes, the surfaces of the specimens remained catalytically active even though the crud layer formed on top of the existing oxide film had a thickness of 1 μm. Hettiarachchi et al. have studied whether the crudding process is catalysed on noble metal coated AISI 304 SS surfaces, but they did not observe any effect.[123]

5.2.5 Possible side effects of noble metal coating

One of the concerns related to the noble metal applications has been that the corrosion potential of Pd/Pt containing surfaces might be higher than the corrosion potential of uncoated materials under excess of oxygen/hydrogen peroxide concentrations in the reactor water. This would lead to higher crack growth rates in BWRs under normal water chemistry conditions during transients from HWC to NWC or during some other intermediate water chemistry conditions.[126] There is some controversy in the results, because the laboratory results done by Kim showed that Pt has higher potentials than the stainless steel samples in excess of oxygen.[116] However, the Pt plate electrodes never exhibited a higher corrosion potential than that of stainless steel samples in in-core ECP measurements, as reported by Andresen.[117] The tests carried out at Halden test reactor have also shown that the crack growth rates of noble metal doped specimens were not higher compared to undoped specimens under NWC conditions.[110]

Another concern has been the corrosion behaviour of fuel cladding material once the NMCA has been applied on the surfaces of reactor core components. Laboratory and some in-core results show that noble metal coating on Zircaloy fuel cladding does not affect the corrosion nor the integrity of the cladding material.[117] However, there are no results if noble metal coating will have an effect on hydride formation in the fuel cladding material. Laboratory tests and modelling

work has also shown that ^{16}N formation on catalytic surface is an insignificant factor.[117]

Once NMCA has been applied, the oxides formed during NWC will start to restructure. This could lead to increased ^{60}Co incorporation into the changing oxides. Plant measurements have shown increased dose rates during shutdowns due to the accumulation of ^{60}Co into the oxides on the recirculation piping after operation under HWC. The reason has been related mainly to the restructuring of the oxide films. On the other hand, the lower potentials cause reduction of oxide films formed under NWC operation, leading possibly again to increased ^{60}Co incorporation into the oxide. However, activity incorporation into the oxide films can be mitigated efficiently by using Zn injections as shown by Lin.[8]

5.3 Application of dielectric oxides on construction materials

There are several unknown parameters in the core of BWR conditioons, such as water flow rates, radiation flux, dissolved hydrogen/oxygen concentrations, etc. A typical location with a poorly defined conditions is the core channel boiling region, where both hydrogen and oxygen are stripped from the liquid to the vapour phase. The concentration of hydrogen peroxide remains high as a result of the water radiolysis and therefore increasing the ECP of the construction materials in this region. Therefore, it is possible that neither HWC nor NMCA can provide sufficient decrease in the ECP of construction materials simply because of very high oxidant concentrations or difficulty in achieving stoichiometric excess of hydrogen. These technologies may also be unattractive to the operators.

Another possibility to reduce susceptibility of stainless steel component to stress corrosion cracking has been proposed by Yeh et al. They have modelled two real cases, in which the corrosion potentials of materials can be decreased in operating BWRs by reducing the exchange current densities of the major redox couples by using dielectric coatings onto the metal surface.[126] Their calculations show that by adopting a general inhibition technique, the reactor components can be protected from IGSCC even without HWC,

as shown in Figure 29.

The calculations shown in Figure 29 simulate the situation in Dresden 2 unit. The top figure clearly shows that the noble metal coating can not protect any parts of the heat transport system under NWC. However, if the oxides on material surfaces are insulating, only the components in core channel (1), core bypass (2) and upper plenum (3) have potentials higher than -230 mV$_{SHE}$. All the other parts are protected from IGSCC. The situation changes when HWC is applied. By using some of the noble metal coating techniques most of the components have low enough potentials. However, due to the intense radiolysis of the water in core channel and upper plenum, the potentials in these regions remain high. A general inhibition method seems to decrease potentials throughout the heat transport system, providing protection against IGSCC even with low hydrogen concentrations. Calculations reported by Yeh et al.
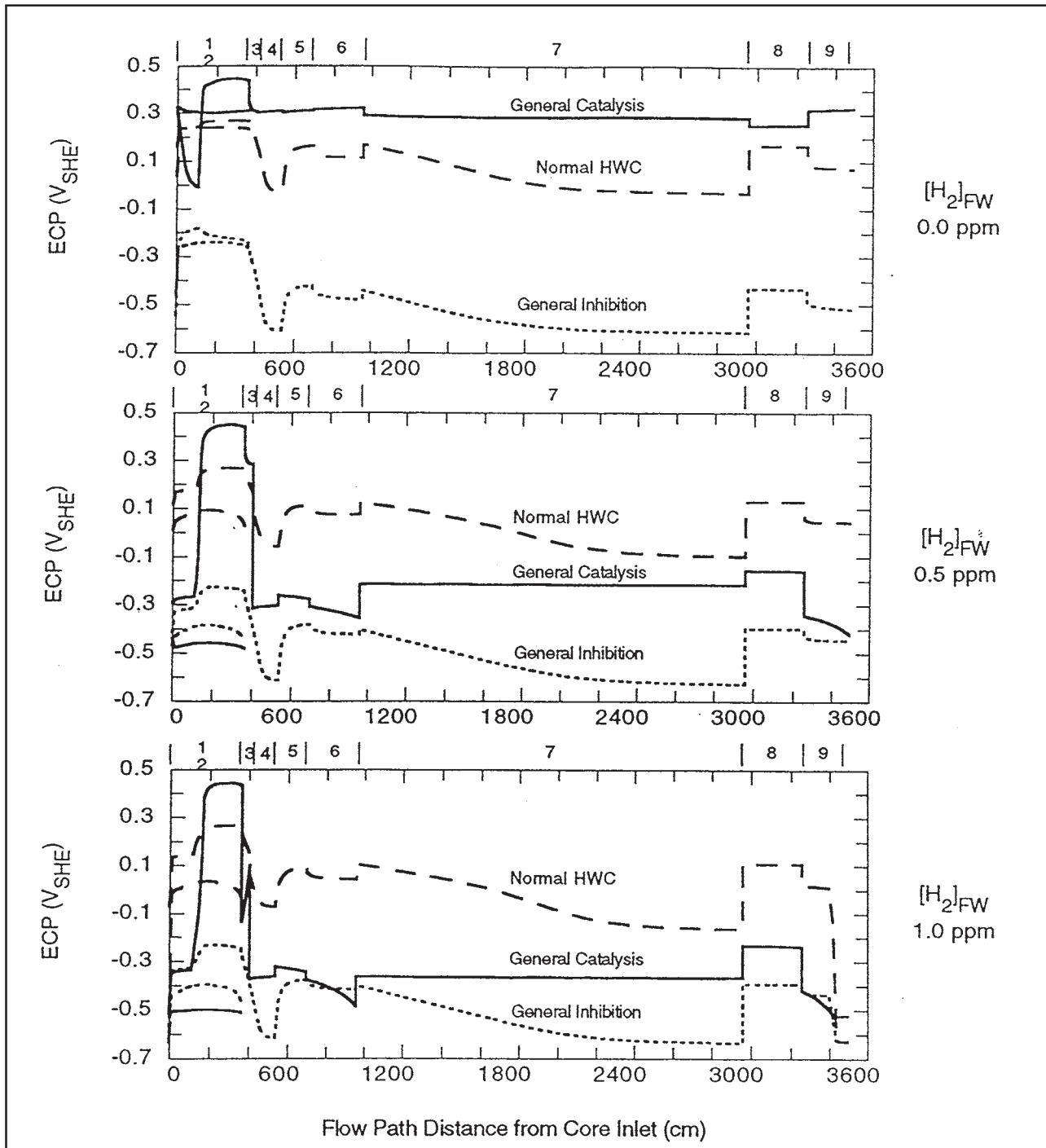

Figure 29. Corrosion potential variation as a function of feed water hydrogen concentration along the heat transport circuit at Dresden-2.[126]

are only qualitative in nature. However, they show that by adopting a general inhibition technique, the reactor components can be protected from IGSCC.

A similar approach was used by Kim et al., who measured the ECPs of materials, which formed an electrically non-conducting oxide film onto the metal surface.[127] This type of films in high temperature water could be obtainable by coating the construction material surfaces or by alloying certain elements, such as Zr and Y, into the base metal. The behaviour of the corrosion potentials of the specimens coated either by plasma spray with yttrium stabilised zirconia (YSZ) or immersed in

water containing 1 mM $ZrO(NO_2)_2$ are shown in Figures 30 and 31. The former specimens behaved like pure Zr having low potentials even at rather high oxygen concentrations.

At oxygen levels higher than 300 ppb ECP started to increase rather rapidly, most likely due to the presence of excessive pores and cracks in the coating. However, when the oxygen concentrations were lower than 180 ppb, the measured ECP was somewhat lower than with untreated samples. At the moment the thermal spray coating seems to provide the most promising approach in lowering the corrosion potential of construction materials below the IGSCC protection potential.
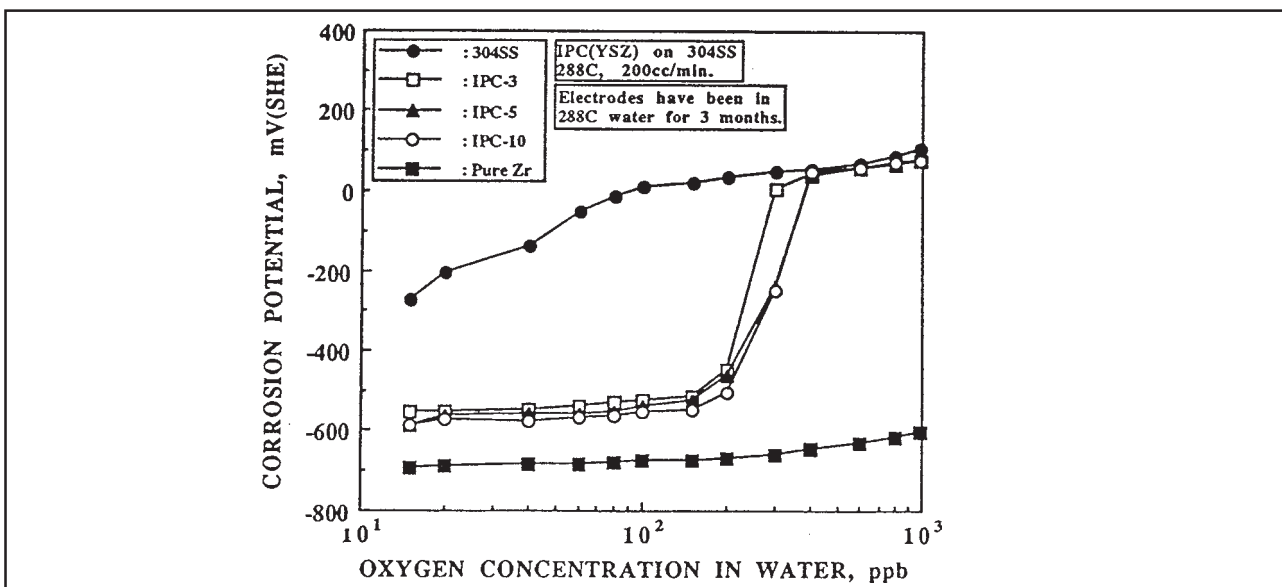
Figures 30. *Corrosion potentials of AISI 304 SS, pure Zr and YSZ coated AISI 304 SS electrodes.[127]*
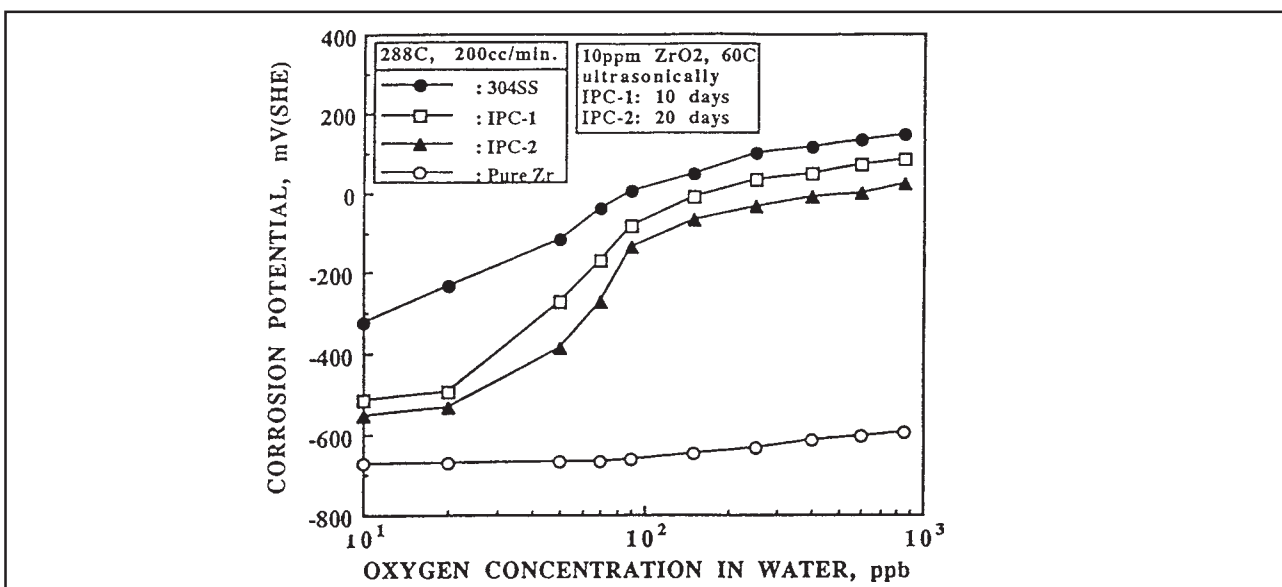

Figure 31. *Corrosion potentials of AISI 304 SS, pure Zr and ZrO2 doped AISI 304 SS electrodes.[127]*

6 SUMMARY AND CONCLUSIONS

The primary coolant oxidises the surfaces of construction materials in nuclear power plants. The oxide films formed in high temperature aqueous solutions generally consist of a compact inner layer and of a more porous outer layer. Although this duplex-film concept is a simplification, it can be used to describe the behaviour of oxide films in different operational environments. In addition to physical differences, the composition and stoichiometry of the oxide films changes gradually with distance from the film/environment interface. The nature of the oxide films influence significantly the extent of incorporation of activated corrosion products into the primary circuit surfaces, which may cause additional occupational doses for the maintenance personnel.

The growth of oxide films and the oxide thickness is determined by the rate of ion transport through the existing oxide and by the extent of saturation of the coolant next to the oxide layer by soluble corrosion products. During deposition of corrosion products, activated species are also incorporated into the oxide films. The incorporation of radioactive cobalt into oxide films can basically proceed via at least three different mechanisms: surface adsorption/complexation, ion-exchange or direct reaction/crystallisation. In addition, diffusion along the pores and cracks in the outer part of the duplex oxide film, as well as diffusion along the grain boundaries in the dense part of the oxide, enables the activity to be spread throughout the oxide film.

Zinc and activity build-up

Injection of zinc into the primary coolant has been shown to decrease the incorporation of activated corrosion products into the existing oxides. Even though the exact mechanisms by which zinc acts are not yet known, it is assumed that Zn may block one of the above mentioned diffusion paths. Zinc may also decrease the defect concentration in the spinel oxide structure by occupying existing defects in the oxide lattice. This should slow down the ion transport though the oxide, leading to a reduced rate of oxide growth and the formation of thinner oxide films. The fact that zinc ion significantly retards the film growth leads automatically to a smaller number of available adsorption sites for ^{60}Co. It is also possible that zinc competes with cobalt for occupancy of surface sites for adsorption and therefore prevents additional ^{60}Co adsorption onto the oxide surface. Zn may also inhibit the ion exchange reactions between inactive cobalt and ^{60}Co on the surfaces leading to lower activity build-up in the oxide. However, this reaction requires a high activation energy and therefore it is relatively unlikely in most cases.

Most of the studies on the effect of Zn have concentrated on observing the physical changes in the oxide film structure. Only little attention has been paid to changes in the electronic and electrochemical properties of the oxide films caused by zinc injections. Even though a significant amount of testing has been carried out, the comparison between the results is tedious, because the experimental arrangements (environments, pH, materials) differ significantly from one test to another.

Zinc and stress corrosion cracking (SCC)

The current models for SCC assume that the anodic and the respective cathodic reactions contributing to crack growth occur partly on or in the oxide films. The crack growth has been explained to take place in the metal by capture of vacancies in the metal close to the crack tip. If most of the vacancies in the metal lattice are generated as a result of the dissolution of the metal through the oxide, the crack growth rate may again be control-

led by the transport rate of species through the oxide film. The decreasing influence of Zn on ion transport may lead to a reduced rate of vacancy production and thus to low crack growth rates. Furthermore, the resulting thinner oxide film is less likely to break and expose the base metal to the environment than a thicker oxide with a higher defect concentration.

The lack of an unambiguous explanation of the effects of zinc on the crack growth rates can be ascribed to the fact that control of the test environments (Zn concentration, pH, conductivity, etc.) differ from one experiment to another. This complicates the interpretation of the results, because usually more than one factor is different between separate tests. On the other hand, the impact of Zn may also be relatively small and longer exposure times may be needed to observe real effects on crack growth rates.

Hydrogen and noble metal water chemistries

Clear decrease in susceptibility of construction materials for the stress corrosion cracking in boiling water reactors can be observed when hydrogen is added into the feed water. Hydrogen addition decreases the levels of oxidising species and thus lowers the corrosion potential (ECP) of the construction materials. Recent plant experiments have shown that by applying the noble metal chemical addition- technique, oxide films on construction materials behave like noble metal surfaces, catalysing the recombination reaction between hydrogen and oxygen. This reaction leads to corrosion potentials low enough to avoid stress corrosion to proceed even with reasonably low hydrogen concentrations. An additional benefit of a lower corrosion potential is higher acceptable impurity levels in the coolant without an effect on the crack growth rates. This provides high tolerance to severe water chemistry transients (e.g. impurity in-leakage). However, to be an economically viable process in operating BWRs, the applied coating should retain the catalytic activity at least for two fuel cycles under the high flow rates of the BWR coolant.

One of the concerns related to the noble metal applications has been that the corrosion potential of Pd/Pt containing surfaces might be higher than the corrosion potential of uncoated materials under excess of oxygen/hydrogen peroxide concentrations in the reactor water. This would lead to higher crack growth rates in BWRs during transients from hydrogen water chemistry (HWC) to NWC or during some other intermediate water chemistry conditions. Therefore, it is possible that neither HWC nor noble metal chemical addition-technique can provide sufficient decrease in the ECP of construction materials.

Dielectric coating on metal surfaces

Another possibility to reduce susceptibility of stainless steel components to stress corrosion cracking is to apply dielectric coatings onto the metal surface. This type of films in high temperature water could be obtained by coating the construction material surfaces using chemical additions into the coolant or by alloying certain elements, such as Zr and Y, into the base metal. By using dielectric coatings techniques, the reactor components can be protected from intergranular stress corrosion cracking even without HWC. It is not yet clear if these techniques can be developed into the stage where real plant experiments will be performed.

Concluding remarks

Although further improvements in water chemistry in NPPs, e.g. zinc dosing and application of noble metal coating technology, have recently been introduced, it is evident that a proper understanding of the interaction of the coolant and the oxide films on material surfaces in NPPs is not yet available. The fundamental questions related to ionic and electronic conduction in the oxide films as well as effects of different reaction rates on the observed phenomena in the oxide films have remained unanswered. Therefore, it is impossible to predict material behaviour in different environmental conditions such as novel water chemistries which involve injection of new chemicals into the primary coolant. More experimental work and modelling in carefully controlled environments is needed to find out the key processes related to the phenomena in oxide films during application of novel water chemistries.

REFERENCES

1   Chantoin P. Coolant technology of water cooled reactors. Volume 3: Activity transport mechanisms in water cooled reactors. IAEA Technical Reports Series No. 667. Vienna: IAEA, 1992.

2   Fox MJ. A review of boiling water reactor water chemistry. NUREG/CR-5115, ANL-88-42, R5. Washington: US Nuclear Regulatory Commission, NRC FIN A2212, 1989.

3   Indig ME, Nelson JL. Electrochemical measurements and modelling predictions in boiling water reactors under various operating conditions. Corrosion 1991;47:202–209.

4   Macdonald DD. Viability of hydrogen water chemistry for protecting in-vessel components of boiling water reactors. Corrosion 1992;48:194–204.

5   Cowan RL, Lin CC, Marble WJ, Ruiz CP. Hydrogen water chemistry in BWRs. Proceedings of Fifth International Symposium on Environmental Degradation of Materials in Nuclear Power Systems—Water Reactors, Monterey, 1991: 50.

6   Macdonald DD, Song H, Mäkelä K, Yoshida K. Corrosion potential measurements on Type 304 SS and Alloy 182 in simulated BWR environments. Corrosion 1993;49:8–17.

7   Jones R. BWR Hydrogen Water Chemistry Guidelines: 1987 Revision. EPRI NP-4947SR. Palo Alto, USA: EPRI, 1988.

8   Lin CC. Hydrogen water chemistry effects on BWR radiation build-up. Vol. 1: Laboratory results and plant data. EPRI TR-104605-V1. Palo Alto, USA: EPRI, 1994.

9   Lister DH. The transport of radioactive corrosion products in high temperature water. II. The activation of isothermal steel surfaces. Nuclear Science and Engineering 1976;59: 406–26.

10 Bergman CA, Durkosh DE, Linday WT, Roesmer J. The role of coolant chemistry in PWR radiation field build-up. EPRI NP-4247. Palo Alto, USA: EPRI, 1985.

11 Polley MV, Garbett K, Pick WE. A survey of the effect of primary coolant pH on Westinghouse PWR plant radiation fields. EPRI TR-104180. Palo Alto, USA: EPRI, 1994.

12 Sweeton FH, Baes CF Jr. The solubility of magnetite and hydrolysis of ferrous ion in aqueous solutions at elevated temperatures. Journal of Chemistry and Thermodynamics 1970;2:479–500.

13 Tremaine PR, LeBlanc JC. Solubility of magnetite and the hydrolysis and oxidation of Fe^{2+} in water to 300 °C. Journal of Solution Chemistry 1980;9:415–28.

14 Kunig RH, Sandler YL. The solubility of simulated PWR primary circuit corrosion products. EPRI NP-4248. Palo Alto, USA: EPRI, 1986.

15 Niedrach LW. Effect of palladium coatings on the corrosion potential of stainless steel in high temperature water containing dissolved hydrogen and oxygen. Corrosion 1991;47:162–169.

16 Wood CJ. PWR primary water chemistry guidelines: Revision 2. EPRI NP-7077. Palo Alto, USA: EPRI, 1990.

17 Rickersten D. PWR zinc injection experience at Farley unit 2. Proceedings of EPRI Radiation Filed Control and Chemical Decontamination Seminar, Tampa, USA, November 1995.

18 Lister DH, Godin MS. The effect of dissolved zinc on the transport of corrosion products in PWRs. EPRI NP-6975-D. EPRI, 1990.

19 Rebak RB, Szklarska-Smialowska Z. About the mechanism of stress corrosion cracking of Alloy 600 in high temperature water. Proceedings of Seventh International Symposium on Environmental Degradation of Materials in Nuclear Power Systems—Water Reactors, Vol 1, Breckenridge Colorado, USA, August 1995: 855–866.

20 Esposito JN, Economy G, Byers WA, Esposito JB, Pement FW, Jacko RJ, Bergmann CA. The addition of zinc to primary reactor coolant for enhanced PWSCC resistance. Proceedings of Fifth International Symposium on Environmental Degradation of Materials in Nuclear Power Systems—Water Reactors, Monterey, USA, August 1991: 495–501.

21 Heslop RB, Jones K. Inorganic chemistry; A guide to advanced studies. Elsevier Scientific Publ. Comp., 1976.

22 Douglas B, McDaniel DHJ, Alexander JJ. Concepts and models of inorganic chemistry. New York: John Wiley & Sons, Inc., 1983.

23 Cotton FA, Wilkinson G. Basic Inorganic Chemistry. New York: John Wiley & Sons, Inc., 1976.

24 Dunn TM, Mclure DS, Pearson RG. "Some aspects of Crystal Field Theory". New York: Harper & Row, 1965.

25 Wells AF. "Structural Inorganic Chemistry". London: Oxford University Press, 1962.

26 Harding JH. Modelling the effects of zinc addition on the uptake of cobalt by oxide films in PWRs. Proceedings of Water Chemistry of Nuclear Reactor Systems, 7, Bournemouth, Great Britain, 1996: 308–316.

27 Durrant PJ. Durrant B. Introduction to advanced inorganic chemistry. London: Longman Group Ltd., 1970.

28 Huheey JE. Principles of structures and reactivity in inorganic chemistry. Harper International SI Edition, 1983.

29 West A. Solid state chemistry and its applications. Wiley, 1985.

30 Kofstad P. High temperature corrosion. London & New York: Elsevier Applied Science, 1988.

31 Rickert H. Electrochemistry of Solids. Springer-Verlag, 1982.

32 Rosenberg HM. The solid state. Oxford Science Publ., Great Britain, 1988.

33 Van Vlack LH. Elements of materials science and engineering. Addison-Wesley Publ. Co., 1989.

34 Robertson J. The mechanism of high temperature aqueous corrosion of stainless steel. Corrosion Science 1991;32(4):443–65.

35 Lister DH. The transport of radioactive corrosion products in high temperature water I. Recirculation loop experiments. Nuclear Science and Engineering 1975;58:239–51.

36   Tapping RL, Davidson RD, MacAlpine E, Lister DH. The composition and morphology of oxide films formed on type 304 stainless steel in lithiated high temperature water. Corrosion Science 1986;26:563–577.

37   Smith-Magowan D. Evaluation of the applicability of colloid studies to Cobalt-60 deposition in LWRs. EPRI NP-3773. Palo Alto, USA: EPRI, 1984.

38   Lister DH, McAlpine E, Tapping RL, Hocking WH. Corrosion-product release in LWRs: 1984–1985 Progress Report. EPRI NP-4741. Palo Alto, USA: EPRI, 1986.

39   Berry WE, Diegle RB. Survey of corrosion product generation, transport, and deposition in light water nuclear reactors. EPRI NP-522. Palo Alto, USA: EPRI, 1979.

40   Asakura Y, Karasawa H, Sakagami M, Uchida S. Relationships between corrosion behaviour of AISI 304 stainless steel in high temperature pure water and its oxide film structures. Corrosion 1989;45:119–124.

41   Hermansson HP, Stigenberg M, Wikmark G. The KEMOX-2000 project: minimising radiation doses by optimising oxide conditions. Proceedings of water chemistry of nuclear reactor systems, 7, Bournemouth, Great Britain, 1996: 141–143.

42   Baston VF, Garbauskas MF, Ocken H. Material characterisation of corrosion films on BWR components exposed to HWC and zinc injections. Proceedings of Water Chemistry of Nuclear Reactor Systems, 7, Bournemouth, Great Britain, 1996: 558–565.

43   Lister DH, Davidson RD, McAlpine E. The mechanism and kinetics of corrosion product release from stainless steel in lithiated high temperature water. Corrosion Science 1987;27(2):113–140.

44   Bogaerts WF, Bettendorf C. Electrochemistry and corrosion of alloys in high-temperature water. EPRI NP-4705. Palo Alto, USA: EPRI, 1986.

45   Sandler YL. Structure of PWR primary corrosion products. Corrosion 1979;35:205–208.

46   Lister DH, Davidson RD. Corrosion product release in light water reactors. EPRI NP-6512. Palo Alto, USA: EPRI, 1989.

47   Lister DH. Activity transport and corrosion processes in PWRs. Proceedings of Sixth Conference on Water Chemistry of Nuclear Reactor Systems, 6, Bournemouth, Great Britain, 1992: 49–60.

48   McIntyre NS, Zetaruk DG. Owen D. X-ray photoelectron studies of the aqueous oxidation of Inconel 600 alloy. Journal of the Electrochemical Society 1979;126:750–760.

49   Schuster E, Neeb KH, Ahlanger W, Henkelmann R, Jarnstrom RT. Analysis of primary side oxide layers on steam generator tubes from PWRs and radiochemical issues on the contamination of primary circuits. Journal of Nuclear Materials 1988;152:1–8.

50   Stellwag B. Growth mechanism of oxide films on austenitic FeCrNi-alloys in high temperature water. Proceedings of International Conference on Interaction of Iron Based Materials with Water and Steam. EPRI TR-102101. Palo Alto, USA, EPRI, 1993: 20/1.

51   Beverskog B, Puigdomenech I. Revised Pourbaix diagrams for chromium at 25–300 °C. Corrosion Science 1997;39:43–57.

52   Lin CC, Smith FR. BWR cobalt deposition studies: Final report. EPRI NP-5808, May. Palo Alto, USA: EPRI, 1988.

53 Kelén T, Hermansson HP. The KEMOX-2000 project: minimising radiation doses by optimising oxide conditions. Proceedings of Water Chemistry of Nuclear Reactor Systems, 7, Bournemouth, Great Britain, 1996: 156–161.

54 Ishigure K, Matsuura C, Mizuochi M, Takahashi M, Isotope exchange processes of cobalt ions on the surfaces of crud particles, Proceedings of Water Chemistry of Nuclear Reactor Systems, 4, Bournemouth, Great Britain, 1986: 145–152.

55 Marble WJ. Control of radiation-field build-up in BWRs. NP-4072, June. Palo Alto, USA: EPRI, 1985.

56 Ocken H, Wood CJ. Status report on radiation exposure reduction at US nuclear power plants. Proceedings of Sixth Conference on Water Chemistry of Nuclear Reactor Systems, 6, Bournemouth, Great Britain, 1992: 1–8.

57 Rickersten D. PWR zinc injection experience at Farley unit 2. Proceedings of EPRI Radiation Filed Control and Chemical Decontamination Seminar, Tampa, USA, November 1995.

58 Stellwag B, Ruehle W, Staudt U. Overview of the VGB project activity build-up in light water reactors, Proceedings of Water Chemistry of Nuclear Reactor Systems, 7, Vol. 2, Bournemouth, Great Britain, 1996: 544–551.

59 Marble WJ, Cowan RL, Wood CJ. Control of cobalt-60 deposition in BWRs, Proceedings of Fourth Conference on Water Chemistry of Nuclear Reactor Systems, 4, Bournemouth, Great Britain, 1986: 113–119.

60 Ocken H, Wood CJ. Radiation-field control manual—1991 Revision. EPRI TR-100265, March. Palo Alto, USA: EPRI, 1992.

61 Marble WJ, Diaz, Levin HA, Garcia SE. Evaluation of recent experience using zinc addition to reduce BWR primary system radiation build-up. EPRI TR-104606, December. Palo Alto, USA: EPRI, 1994.

62 Marble WJ, Cowen RL. Mitigation of radiation buildup in the BWR by feed water zinc addition. Proceedings of JAIF International Conference on Water Chemistry in Nuclear Power Plants—Operational Experience and Strategy for Technical Innovation. Fukui City, Japan, April 22–25, 1991: 55–65.

63 Puyane R. Effectiveness of isotope depleted ZnO to minimize radiation build-up in boiling water nuclear reactors. Journal of Materials Processing Technology 1996;56:863–872.

64 Kelén T, Lundgren K. Chemistry and materials impact on activity build-up in BWRs—general conclusions from BKM-crud computer simulation studies. Proceedings of Conference on Chemistry in Water Reactors: Operating Experience & New Developments. Nice, France, 1994: 263–270.

65 Haginuma, Effect of zinc addition on cobalt ion accumulation into the corroded surface of type 304 SS in high temperature water. Proceedings of Water Chemistry of Nuclear Reactor Systems, 7, Bournemouth, Great Britain, 1996: 128–130.

66 Permer L, Österlundh CG. Experimental study of cobalt uptake by trevorite and chromite with and without the presence of zinc. Proceedings of Water Chemistry of Nuclear Reactor Systems, 7, Bournemouth, Great Britain, 1996: 122–125.

67 Niedrach LW, Stoddard WH. Effect of zinc on corrosion films that form on stainless steel. Corrosion;1986;42(9):546–549.

68 Byers WA, Jacko RJ, The influence of zinc addition and PWR primary water chemistry on surface films that form on nickel base alloys and stainless steel. Sixth International Symposium on Environmental Degradation of Materials in Nuclear Power Systems—Water Reactors, 1993: 837–844.

69 Baston VF, Garbauskas MF, Bozeman, J. Decontamination flange film characterisation for a boiling water reactor under hydrogen water chemistry, Journal of Nuclear Technology 1996;114:339–349.

70 Haginuma M, Ono S, Kumagai M, Takamori K, Tachibana K, Ishigure K. Cobalt deposition control by zinc and hydrogen injection in BWR environment. Proceedings of Conference on Chemistry in Water Reactors: Operating Experience & New Developments. Nice, France, 1994: 386–389.

71 Beverskog B, Puigdomenech I. Revised Pourbaix diagrams for zinc at 25–300 °C. Corrosion Science 1997;39:107–113.

72 Hanzawa Y, Ishigure K, Matsuura C, Hiroishi D. The effect of zinc addition on cobalt accumulation on steel surfaces and its thermodynamics. Proceedings of Water Chemistry of Nuclear Reactor Systems, 7, Vol. 2, Bournemouth, UK, 1996: 301–308.

73 Allsop HA. The benefits of zinc addition to primary side coolant. Proceedings of Conference on Chemistry in Water Reactors: Operating Experience & New Developments. Nice, France, 1994: 321–327.

74 Walker ZH, Allsop HA, Godin MSL, Sawicki JA, Turner CW, Klimas SJ. Effects of zinc additions under Candu pressurised heavy water reactor conditions. Proceedings of Water Chemistry of Nuclear Reactor Systems, 7, Vol. 2, Bournemouth, UK, 1996: 552–557.

75 Bennet PJ, Gunnerud P, Loner H, Pettersen, Harper A. The effect of zinc addition on cobalt deposition in PWRs, Proceedings of Water Chemistry of Nuclear Reactor Systems, 7, Vol. 2, Bournemouth, UK, 1996: 293–300.

76 Pathania R, Yagnik S, Gold RE, Dove M, Kolstad E. Evaluation of zinc addition to PWR primary coolant. Proceedings of Seventh International Symposium on Environmental Degradation of Materials in Nuclear Power Systems—Water Reactors, Vol. 1. Breckenridge, Colorado, USA, August 1995: 163–173.

77 Bergmann, RE, Gold RE, Sejvar, JD, Perock JD, Dove M. Overview of zinc addition in the Farley 2 reactor. Proceedings of Water Chemistry of Nuclear Reactor Systems 7, Vol. 2, Bournemouth, UK, 1996: 287–292.

78 Nieder D, Wolter D. Einführung der Zink-Dosierung in KWB-B. Proceedings of VGB Meeting on Water Chemistry in NPPs. Essen, Germany, 1997: 1–7.

79 Hsueh R, Kohse G, Harling OK. In-reactor study of zinc injection to reduce radioactive corrosion product transport in PWRs. Am. Nuclear Society Transactions: 151–152.

80 Riess R, Stellwag B. Effects of zinc on the contamination and structure of oxide layers. Proceedings of Water Chemistry of Nuclear Reactor Systems, 7, Vol. 2, Bournemouth, Great Britain, 1996: 573–582.

81 Korb J, Stellwag B. Thermodynamics of zinc chemistry in PWRs-effects and alternatives to zinc. Proceedings of Water Chemistry of Nuclear Reactor Systems, 7, Bournemouth, Great Britain, 1996: 147–49.

82 Bennet P. The longer term effects of zinc addition on cobalt deposition in PWRs. HWR-477. Halden, Norway, 1996.

83   Bennet P. The effects of zinc on cobalt deposition in PWRs: Summary Report. HWR-450. Halden, Norway, 1996.

84   Bennet P. Incorporation of zinc into oxide films in PWRs. HWR-489. Halden, Norway, 1996.

85   Mäkelä K. Activity incorporation into zinc doped PWR oxides. HWR-557. To be published at Enlarged Halden Programme Group Meeting at Lillehammer, March 1997.

86   Gold RE, Byers WA, Jacko RJ. Zinc-oxide corrosion film interactions in PWR primary coolant. SFEN, Fontevraud, France: 300–309.

87   Osato T, Hemmi Y. Corrosion and Co uptake behaviour on structural material in BWR primary coolants at Zn and Ni addition. Proceedings of Water Chemistry of Nuclear Reactor Systems, 7, Bournemouth, Great Britain, 1996: 125–127.

88   Ullberg M. Iron to nickel ratio of BWR fuel crud - effects and interpretation. Proceedings of Water Chemistry of Nuclear Reactor Systems, 7, Vol. 2, Bournemouth, Great Britain, 1996: 496–501.

89   Aizawa M, Ohsumi K, Asakura Y, Morikava Y, Hirahara Y, Sakai T, Harguchi K, Operating experience of Japanise improvement and standardisation BWRs and behaviour of radioactivity in reactor water, Proceedings of Sixth Conference on Water Chemistry of Nuclear Reactor Systems, 6, Bournemouth, Great Britain, 1992: 39–44.

90   Uetake N, Hosakawa H, Uchida S, Ohsumi K, Tone T, Suzuki N. Development of water chemistry optimisation technologies in recent Japanese BWRs. Proceedings of Water Chemistry of Nuclear Reactor Systems, 7, Bournemouth, Great Britain, 1996: 168–175.

91   Cheng BC, Turnage KG, Hudson M, Brown JM, Armstrong EA. Fuel performance and water chemistry variables in LWRs. Proceedings of 1997 International Topical Meeting on Light Water Reactor Fuel Performance, Portland, Canada: 379–388.

92   Levin HA, Gercia SE, BWR fuel experience with zinc injection, Proceedings of Seventh International Symposium on Environmental Degradation of Materials in Nuclear Power Systems—Water Reactors. Vol. 2. Breckenridge, Colorado, USA, August, 1995: 1217–1230.

93   Cheng BC, Turnage KG, Hudson M, Brown JM, Armstrong EA. Fuel performance and water chemistry variables in LWRs. Proceedings of 1997 International Topical Meeting on Light Water Reactor Fuel Performance, Portland, Canada: 379–388.

94   Aomi M, Kogai T, Shimada S, Ichikawa N, Ibe E, Ishii Y, Cheng B, Lutz D. Evaluation of Zircaloy corrosion under various water chemistries in a BWR simulation loop, Proceedings of Water Chemistry of Nuclear Reactor Systems, 7, Bournemouth, Great Britain, 1996: 284–286.

95   Baston VF, Indig ME, Skarpelos JM, BWR chromium chemistry. EPRI TR-100792, October. EPRI: Palo Alto, USA, 1992.

96   Ljungberg L, Halldén E. BWR water chemistry impurity studies: literature review of effects on stress corrosion cracking: Interim Report EPRI NP-3663. EPRI: Palo Alto, USA.

97   Macdonald DD, Urquidi-Macdonald M. A coupled environment model for stress corrosion cracking in sensitised type 304 stainless steel in LWR environments. Corrosion Science 1991;32:51–81.

98 Galvele JR. Electrochemical aspects of stress corrosion cracking. In: White, RE et al (Eds.) Modern Aspects of Electrochemistry, No. 27. New York: Plenum Press.

99 Andresen PL. SCC growth rate behaviour in BWR water of increased purity. 8th International Symposium on Environmental Degradation of Materials in Nuclear Power Systems—Water Reactors, Amelia Island, USA, August 10–14, 1997: 603–614.

100 Turnbull A. Modelling of environment assisted cracking. Corrosion Science 1993;34:921–960.

101 Sarver JM, Pathania RS, Stuckey K, Fyftch S, Gelpi A, Foucault M, Hunt ES. Stress corrosion cracking of welded Alloy 600 penetration mockups. Proceedings of Seventh International Symposium on Environmental Degradation of Materials in Nuclear Power Systems—Water Reactors, Vol. 1, Breckenridge, Colorado, USA, August 1995: 13–24.

102 Rebak RB, Szklarska-Smialowska Z. Effect of partial pressure of hydrogen on IGSCC of alloy 600 in PWR primary water. Corrosion 1991;47:754–757.

103 Galvele JR. Electrochemical aspects of stress corrosion cracking. In: White, RE et al. (Eds.) Modern Aspects of Electrochemistry, No 27. New York: Plenum Press, 1995: 233–358.

104 Lagerström, J, Ehrnstén, U, Saario, T, Laitinen, T, Hänninen, H. Model for environmentally assisted cracking of Alloy 600 in PWR primary water. Proceedings of the Eighth International Symposium on Environmental Degradation of Materials in Nuclear Power Systems—Water Reactors, Florida, August 10–14, 1997: 349–356.

105 Airey GP, Allan SJ, Angell MG. The effect of zinc on the stress corrosion cracking of Inconel alloys. Proceedings of Water Chemistry of Nuclear Reactor Systems, 7, Bournemouth, Great Britain, 1996: 478–482.

106 Congleton J, Yang W. The effect of applied potential on the stress corrosion cracking of sensitized type 316 stainless steel in high temperature water. Corrosion Science 1995; 37:429–444.

107 Andresen PL, Diaz TP. Effects of zinc additions on the crack growth rate of sensitised stainless steel and alloys 600 and 182 in 288 °C water. Proceedings of Sixth Conference on Water Chemistry of Nuclear Reactor Systems, 6, Vol. 1, Bournemouth, Great Britain, 1992: 169–175.

108 Andresen PL, Angeliu TM. Effects of zinc addition on the stress corrosion crack growht rate of sensitised stainless steel, alloy 600 & alloy 182 weld metal in 288 °C water. Corrosion 95, USA. Paper 95409.

109 Hettiarachchi S, Wozadlo GP, Diaz TP. Influence of zinc additions on the intergranular stress corrosion crack initiation and growth of sensitised stainless steel in high temperature water. Corrosion 95, USA, Paper 410.

110 Hettiarachchi S, Wozadlo GP, Andresen PL, Diaz TP, Cowan RL. The concept of noble metal chemical addition technology for IGSCC mitigation of structural materials. Proceedings of Seventh International Symposium on Environmental Degradation of Materials in Nuclear Power Systems—Water Reactors, Vol. 1, Breckenridge Colorado, USA, August, 1995: 735–746.

111 Angeliu TM, Andresen PL. The effect of zinc additions on the oxide rupture strain and repassivation kinetics of Fe-based alloys in 288 °C water. Corrosion 1996;52:28–35.

112 Angeliu TM, Andresen PL, Pollick ML. Repassivation and crack propagation of Alloy 600 in 288 °C water. Corrosion 1997;53:114–119.

113 Angeliu TM, Andresen PL. The effect of zinc additions on the oxide rupture strain and repassivation kinetics of Fe-based alloys in 288 °C water. Corrosion 95, Paper 95411, USA.

114 Andresen PL. Effect of noble metal coating & alloying on the stress corrosion crack growth rate of stainless steel in 288 °C water. Proceedings of Sixth International Symposium on Environmental Degradation of Materials in Nuclear Power Systems—Water Reactors, 1993: 245–253.

115 Cowan RL. The mitigation of IGSCC of BWR internals with hydrogen water chemistry. Proceedings of Water Chemistry of Nuclear Reactor Systems, 7, Bournemouth, Great Britain, 1996: 196–206.

116 Kim YJ, Niedrach LW, Andresen PL. Corrosion potential behaviour of noble metal modified alloys in high temperature water. Corrosion 95, Paper 95099, USA.

117 Andresen PL. Application of noble metal technology for mitigation of stress corrosion cracking in BWRs. Proceedings of Seventh International Symposium on Environmental Degradation of Materials in Nuclear Power Systems—Water Reactors, Vol. 1, Breckenridge Colorado, USA, August 1995: 563–577.

118 Andresen PL, Angeliu T. The effect of in-situ noble metal chemical addition on crack growth rate behaviour of structural materials in 288 °C water. Corrosion 96, Paper 96084, USA.

119 Kim Y-J, Andresen PL, Gray DM, Lau YC, Offer HP. Corrosion potential behaviour in high temperature water of noble metal doped alloys coatings deposited by underwater thermal spraying. Proceedings of Seventh International Symposium on Environmental Degradation of Materials in Nuclear Power Systems—Water Reactors, Vol. 1, Breckenridge Colorado, USA, August 1995: 723–734.

120 Kim YJ, Andresen PL, Gray DM, Lau YC, Offer HP. Corrosion potential behaviour in high temperature water of noble metal doped alloys coatings deposited by underwater thermal spraying. Corrosion 1996;52:440–446.

121 Kim YJ, Niedrach LW, Andresen PL. Corrosion potential behaviour of noble metal-modified alloys in high temperature water. Corrosion 1996;52:738–743.

122 Andresen PL. Mitigation of stress corrosion cracking by underwater thermal spray coating of noble metals. Corrosion 95, USA, Paper 95412.

123 Hettiarachchi S, Wozadlo GP, Diaz TP. Long-term performance of noble metal doped surfaces in simulated BWR environments. Corrosion 96, USA, Paper 96099.

124 Kim YJ, Andresen PL, Angeliu TM. In-situ noble metal deposition and its durability on the catalytic response of stainless steel surfaces in high temperature water. Corrosion 96, USA, Paper 96109.

125 Kim YJ, Andresen PL. Effect of zinc and copper additions on catalytic response of noble metal alloyed 304 SS in high temperature water. Corrosion 97, USA, Paper 97112.

126 Yeh TK, Macdonald DD. Predictions of enhancing hydrogen water chemistry for boiling water reactors by general catalysis and general inhibition. Corrosion 96, USA, Paper 96124.

127 Kim YJ, Andresen PL. Application of insulated protective coatings for reduction of corrosion potential in high temperature water. Corrosion 96, USA, Paper 96105.